Investigating B_s three-body decays of scalar mesons in perturbative QCD approach

Hong Yang[*] and Xian-Qiao Yu[†]

School of Physical Science and Technology, Southwest University, Chongqing 400715, China

In this study, we investigate the branching ratios of $B_s^0 \to a_0(980)[\to K\bar{K}, \pi\eta]a_0(980)$, $B_s^0 \to f_0(980)[\to \pi^+\pi^-, K^+K^-]f_0(980)$, and $B_s^0 \to f_0(500)[\to \pi^+\pi^-]f_0(500)$ decays in the pQCD approach, wherein the scalar mesons $a_0(980)$, $f_0(980)$, and $f_0(500)$ are regarded as the lowest-lying $q\bar{q}$ state. In the $SU(3)$ nonet, there exists a mixing between the scalars $f_0(980)$ and $f_0(500)$. Thus, we have considered the mixing effect in our calculations to obtain reliable data, and set the mixing angle θ as [15°, 82°] and [105°, 171°]. Based on the isospin symmetry, we estimated the branching ratios of the $B_s^0 \to f_0(980)[\to \pi^0\pi^0]f_0(980)$ and $B_s^0 \to f_0(500)[\to \pi^0\pi^0]f_0(500)$ decays. The branching ratios of the $B_s^0 \to a_0(980)[\to K\bar{K}, \pi\eta]a_0(980)$ decays are much small, while those of the $B_s^0 \to f_0(980)[\to \pi\pi, K\bar{K}]f_0(980)$ and $B_s^0 \to f_0(500)[\to \pi\pi]f_0(500)$ decays are at the order of 10^{-6}–10^{-5}, which can be tested in the LHCb and Belle II experiments, hopefully.

I. INTRODUCTION

The scalar mesons $a_0(980)$ and $f_0(980)$ have attracted immense attention since their discovery. These scalar mesons, as a key problem in the nonperturbative QCD [1], play a crucial role in understanding the chiral symmetry and confinement in the low-energy region. However, the mysterious internal structure of the scalar mesons $a_0(980)$ and $f_0(980)$ remains a puzzle, many related researches have been carried out accordingly. It has been raised that the scalar mesons $f_0(500)$, $K^*(700)$, $f_0(980)$, and $a_0(980)$ form a $SU(3)$ flavor nonet, whereas the scalars above 1 GeV, including $f_0(1370)$, $a_0(1450)$, $K^*(1430)$, and $f_0(1500)$, form a different nonet [2]. In Ref. [3], two scenarios have been proposed to describe the quark components of the light scalar mesons. According to the first scenario, the light scalar mesons contained in the first $SU(3)$ flavor nonet are the lowest-lying $q\bar{q}$ state. In the other scenario, the scalars in the second nonet are treated as the $q\bar{q}$ state, and the scalar mesons below or close to 1 GeV are considered to be the four-quark bound state. In addition, the presence of nonstrange and strange quark contents in $f_0(980)$ and $f_0(500)$ have been confirmed experimentally; thus, they can be regarded as a mixture of $s\bar{s}$ and $(u\bar{u} + d\bar{d})/\sqrt{2}$ [4]. The aforementioned studies provide a positive significance to explore the internal structure of the scalar mesons.

The perturbative QCD (pQCD) approach based on the k_T factorization has been extensively used to study the decay of B mesons [5–9]. It is well known that the QCD dynamics of the three-body decay is more complex than those of the two-body decay. In the pQCD approach, the three-body decay is usually simplified to a two-body decay by introducing two-hadron distribution amplitudes [10,11], which can be called quasi-two-body decay, containing both resonance and nonresonance information. The dominant contributions are from the parallel motion region, where the invariant mass of the light meson pair is below $O(\bar{\Lambda}M_B)$, and $\bar{\Lambda} = M_B - m_b$ is the difference in mass between the B meson and b quark. Hence, the pQCD factorization formula for the three-body decay amplitude of the B meson is written as [12,13]

$$\mathcal{A} = \mathcal{H} \otimes \phi_B \otimes \phi_{h_3} \otimes \phi_{h_1 h_2}, \tag{1}$$

where the hard decay kernel $\mathcal{H}$ can be calculated by using the perturbative theory. The nonperturbative inputs ϕ_B, $\phi_{h_1 h_2}$ and ϕ_{h_3} are the distribution amplitudes of B meson, $h_1 h_2$ pair and h_3, respectively.

In the past few decades, several B decays with a final state $a_0(980)$ or $f_0(980)$ have been observed in experiments [14–16], and the corresponding theoretical calculations have also attracted increased attention. In Ref. [17,18], the $B_s \to f_0(980)$ transition form factors have been estimated, and the authors still predict the branching ratio of an interesting decay mode $B_s \to J/\psi f_0(980)$. At the same time, the light scalar mesons also can make contributions to the B meson decays as intermediate resonance.

---

[*]15116233293@163.com
[†]yuxq@swu.edu.cn

For example, the LHCb Collaboration reported the $B^0 \to J/\psi K^+ K^-$ decay with the $a_0(980)$ resonance [19], and the Belle Collaboration observed the $B^\pm \to K^\pm f_0(980) \to K^\pm \pi^\mp \pi^\pm$ where the scalar meson $f_0(980)$ was regarded as the intermediate resonance [20]. Recently, many works have been carried out to calculate the three-body decays of the B meson with $a_0(980)$ or $f_0(980)$ resonance in the pQCD approach. In Ref. [21], the branching ratios of the $B \to J/\psi(K\bar{K}, \pi\eta)$ decays have been calculated with the contributions of the scalars $a_0(980)$ and $a_0(1450)$, in which the timelike form factors of $a_0(980)$ resonance and $a_0(1450)$ resonance are shaped by the Flatté model and the Breit-Wigner formula, respectively. The authors of Ref. [22], employing $a_0(980)$, $a_0(1450)$ and $a_0(1950)$ as resonances, analyze the quasi-two-body $B \to a_0(\to K\bar{K}, \pi\eta)h$ decays within the two scenarios mentioned in the first paragraph. In Ref. [23] and Ref. [24], the branching ratios of the $B \to K(\mathcal{R} \to K^+K^-)$ and $B_{(s)} \to V\pi\pi$ decays with $f_0(980)$ resonance have been studied severally by considering the mixing of $s\bar{s}$ and $(u\bar{u} + d\bar{d})/\sqrt{2}$. Furthermore, the authors of Ref. [25] explore the branching ratios and CP violations of the two-body decay $B_s^0 \to SS(a_0(980), f_0(980), f_0(500))$ in the pQCD approach for the first time, and the branching ratios are at the order of $10^{-4} \sim 10^{-6}$ with a high probability to be tested experimentally in the future. Therefore, we further develop the work in Ref. [25]. In our calculation, we regard the scalar mesons $a_0(980)$ and $f_0(980)$ as the $q\bar{q}$ state, just as mentioned in the first scenario, and predict the branching ratios of the quasi-two-body decays $B_s^0 \to S[\to P_1 P_2]S$, where S denotes the light scalar mesons $a_0(980)$, $f_0(980)$, and $f_0(500)$,[1] and $P_1 P_2 = \pi\eta, \pi\pi, K\bar{K}$ is the final state meson pair. For the scalar mesons $f_0(980)$ and $f_0(500)$, we also adopt the corresponding mixing mechanism. The results presented in this paper can be validated in the LHCb and Belle II experiments in the near future.

The rest of this paper is organized as follows. In Sec. II, the theoretical framework of the pQCD, the wave functions involved in the calculations and the helicity amplitudes for the $B_s^0 \to S[\to P_1 P_2]S$ decays are described. In Sec. III, the numerical results are presented and discussed. In Sec. IV, a summary of this work is provided. And the explicit formulas of all the helicity amplitudes are presented in the Appendix.

II. THE THEORETICAL FRAMEWORK AND HELICITY AMPLITUDES

A. The wave functions

The relevant weak effective Hamiltonian of the quasi-two-body $\bar{B}_s^0 \to S[\to P_1 P_2]S$ decays can be written as [26]

---

[1]a_0, f_0, and σ refer to $a_0(980)$, $f_0(980)$, and $f_0(500)$, respectively, in the following text.

$$\mathcal{H}_{\text{eff}} = \frac{G_F}{\sqrt{2}} \left\{ V_{ub} V_{us}^* [C_1(\mu)O_1(\mu) + C_2(\mu)O_2(\mu)] \right.$$
$$\left. - V_{tb} V_{ts}^* \left[\sum_{i=3}^{10} C_i(\mu)O_i(\mu) \right] \right\}, \quad (2)$$

with the Fermi constant $G_F = 1.66378 \times 10^{-5}$ GeV^{-2}, the local four-quark operator $O_i(\mu)$, the corresponding Wilson coefficient $C_i(\mu)$, and $V_{ub}V_{us}^*$ and $V_{tb}V_{ts}^*$ are Cabibbo-Kobayashi-Maskawa (CKM) factors. The Feynman diagrams involved in this work are illustrated in Fig. 1.

Based on the light-cone coordinates, we let the $\bar{B}_s^0$ meson stay at rest, and choose the $P_1 P_2$ meson pair and the final-state S movement along the direction of $n = (1, 0, 0_T)$ and $v = (0, 1, 0_T)$, respectively. So the $\bar{B}_s^0$ meson momentum p_B, the total momentum $p = p_1 + p_2$ of the $P_1 P_2$ meson pair, and the momentum p_3 of the final-state S are considered as

$$p_B = \frac{M_B}{\sqrt{2}}(1, 1, 0_T),$$
$$p = \frac{M_B}{\sqrt{2}}(1 - r^2, \eta, 0_T),$$
$$p_3 = \frac{M_B}{\sqrt{2}}(r^2, 1 - \eta, 0_T), \quad (3)$$

where M_B is the mass of B_s^0, $r = \frac{m_S}{M_B}$ is the mass ratio, m_S refers to the mass of the final-state S. We think the variable $\eta = \omega^2/(M_B^2 - m_S^2)$, and ω is the invariant mass of the $P_1 P_2$ meson pair, which satisfies the relation $\omega^2 = p^2$. Meanwhile, we define $\zeta = p_1^+/p^+$ as one of the $P_1 P_2$ meson pair's momentum fractions. Accordingly, the kinematic variables of other components in the meson pair can be expressed as

$$p_1^- = \frac{M_B}{\sqrt{2}}(1 - \zeta)\eta,$$
$$p_2^+ = \frac{M_B}{\sqrt{2}}(1 - \zeta)(1 - r^2),$$
$$p_2^- = \frac{M_B}{\sqrt{2}}\zeta\eta. \quad (4)$$

We adopt x_B, z, x_3 to indicate the momentum fraction of the light quark in each meson with the range from zero to unity. So the light quark's momentum of the $\bar{B}_s^0(k_B)$, $P_1 P_2(k)$, and $S(k_3)$ are read as

$$k_B = \left(0, \frac{M_B}{\sqrt{2}}x_B, k_{BT}\right),$$
$$k = \left(\frac{M_B}{\sqrt{2}}z(1 - r^2), 0, k_T\right),$$
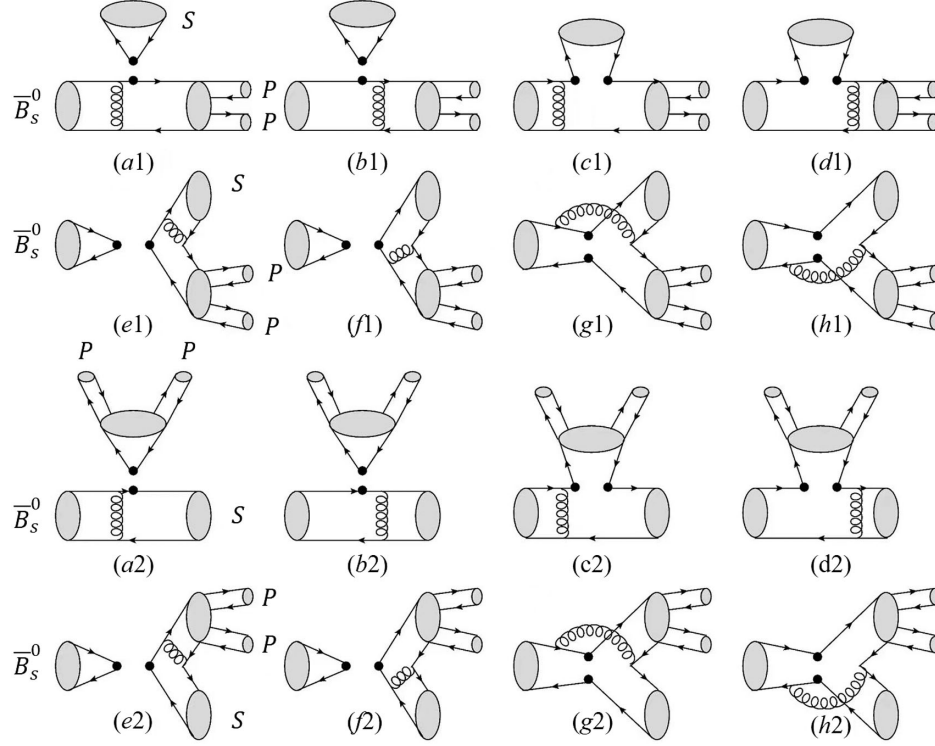$$k_3 = \left(\frac{M_B}{\sqrt{2}}r^2 x_3, \frac{M_B}{\sqrt{2}}(1 - \eta)x_3, k_{3T}\right). \quad (5)$$

FIG. 1.   The Feynman diagrams for the $\bar{B}_s^0 \to S[S \to]P_1 P_2$ decays in pQCD. The symbol black filled circle stands for the weak vertex, S means the scalar mesons, and $P_1 P_2$ denotes the final state meson pair, the corresponding relationships are $a_0(\pi\eta, K\bar{K})$, $f_0(\pi\pi, K\bar{K})$, and $\sigma(\pi\pi)$.

In this work, the wave function of the hadron B_s^0 can be given by Refs. [27–30]

$$\Phi_{B_s} = \frac{i}{\sqrt{2N_c}}(\not{p}_B + M_B)\gamma_5 \phi_{B_s}(x_B, b_B), \qquad (6)$$

where $N_c = 3$ is the color factor, and the distribution amplitude(DA) $\phi_{B_s}(x_B, b_B)$ is expressed in the usual form, which is

$$\phi_{B_s}(x_B, b_B) = N_B x_B^2 (1 - x_B)^2 \exp\left[-\frac{M_B^2 x_B^2}{2\omega_b^2} - \frac{1}{2}(\omega_b b_B)^2\right]; \qquad (7)$$

the factor N_B can be calculated by the normalization $\int_0^1 \phi_{B_s}(x_B, b_B = 0)dx = f_B/(2\sqrt{2N_c})$ with the B_s^0 meson decay constant f_B. And we select the shape parameter $\omega_b = 0.50 \pm 0.05$ GeV [31].

For the light scalar mesons $a_0(980)$ and $f_0(980)$, the wave function can be found in Refs. [3,32],

$$\Phi_S(x_3) = \frac{1}{2\sqrt{2N_c}}[\not{p}_3 \phi_S(x_3) + m_S \phi_S^S(x_3) + m_S(\not{\nu}\not{\eta} - 1)\phi_S^T(x_3)], \qquad (8)$$

with the twist-2 distribution amplitude ϕ_S, which can be expanded by the Gegenbauer polynomials [3,32]:

$$\phi_S(x_3, \mu) = \frac{3}{\sqrt{2N_c}} x_3 (1 - x_3)\left\{f_S(\mu) + \bar{f}_S(\mu)\right.$$
$$\left. \times \sum_{m=1,3}^{\infty} B_m(\mu) C_m^{3/2}(2x_3 - 1)\right\}, \qquad (9)$$

ϕ_S^S and ϕ_S^T are the twist-3 distribution amplitudes, their asymptotic forms can be written as

$$\phi_S^S(x_3, \mu) = \frac{1}{2\sqrt{2N_c}}\bar{f}_S(\mu), \qquad (10)$$

$$\phi_S^S(x_3, \mu) = \frac{1}{2\sqrt{2N_c}}\bar{f}_S(\mu)(1 - 2x_3), \qquad (11)$$

where B_m is the Gegenbauer moment, $C_m^{3/2}(2x_3 - 1)$ denotes the Gegenbauer polynomials, f_S and $\bar{f}_S$ stand for the vector and scalar decay constants of the light scalar mesons a_0 and f_0, respectively. It is obvious that only the odd Gegenbauer moments are considered in the DA of ϕ_S, the even Gegenbauer coefficients B_m are suppressed because of the conservation of charge conjugation invariance or vector current, and we just notice the Gegenbauer moments B_1 and B_3 since the small contribution of higher order Gegenbauer moments can be ignored. On the basis of QCD sum rules with the default scale $\mu = 1$ GeV, for the light scalar meson a_0 [3,32], we adopt the Gegenbauer

moments $B_1 = -0.93 \pm 0.10$ and $B_3 = 0.14 \pm 0.08$, and the scalar decay constant value of which can be taken as $\bar{f}_{a_0} = 0.365 \pm 0.020$. Meanwhile, the Gegenbauer moments and scalar decay constants of the scalar meson f_0 can be listed as [3,32]

$$\bar{f}_S = \bar{f}^n_{f_0} = \bar{f}^s_{f_0} = 0.370 \pm 0.020 \text{ GeV},$$
$$B^n_1 = -0.78 \pm 0.08, \qquad B^n_3 = 0.02 \pm 0.07,$$
$$B^s_{1,3} = 0.8B^n_{1,3}. \tag{12}$$

Here, we take the same value of the two decay constants $\bar{f}^n_{f_0}$ and $\bar{f}^s_{f_0}$ [3]. In this article, we select the vector decay constants $f_S = 0$ due to the discussions in Ref. [25].

For the distribution amplitudes of the final-state P_1P_2 meson pair, we adopt the consistent form of the S-wave pion pair [13,33,34]:

$$\Phi^S_{P_1P_2} = \frac{1}{\sqrt{2N_c}}[\not{p}\phi_S(z,\zeta,\omega^2) + \omega\phi^s_S(z,\zeta,\omega^2) + \omega(\not{n}\not{v} - 1)\phi^t_S(z,\zeta,\omega^2)], \tag{13}$$

where the leading-twist distribution amplitude ϕ_S and the twist-3 DAs ϕ^s_S and ϕ^t_S have similar expression forms as the corresponding twists of the light scalar meson obtained using the timelike form factor by replacing the original scalar decay constants. The asymptotic expression of the light-cone distribution amplitudes $\phi^{(s,t)}_S$ are as follows [21,33]:

$$\phi_S(z,\zeta,\omega^2) = \frac{9F_S(\omega)}{\sqrt{2N_c}}a_2z(1-z)(1-2z),$$
$$\phi^s_S(z,\zeta,\omega^2) = \frac{F_S(\omega)}{2\sqrt{2N_c}},$$
$$\phi^t_S(z,\zeta,\omega^2) = \frac{F_S(\omega)}{2\sqrt{2N_c}}(1-2z), \tag{14}$$

with the Gegenbauer moment $a_2 = 0.3 \pm 0.1$ for a_0 and $a_2 = 0.3 \pm 0.2$ for f_0 [19,35]. $F_S(\omega)$ is the timelike form factor, which can be described well in terms of the relative Breit-Wigner [36]. However, for the a_0 (or f_0) resonance, the main decay channels are $\pi\eta(\pi\pi)$ and $K\bar{K}$. The relative Breit-Wigner line shape cannot be well adapted to the timelike form factor of a_0 and f_0, because both of the a_0 and f_0 resonances are very close to the $K\bar{K}$ threshold, which greatly influences the resonance shape. As such, we choose the widely accepted prescription proposed by Flatté [37], which is given as [21]

$$F^{a_0}_S(\omega) = \frac{C_{a_0}m^2_{a_0}}{m^2_{a_0} - \omega^2 - i(g^2_{\pi\eta}\rho_{\pi\eta} + g^2_{K\bar{K}}\rho_{K\bar{K}})}, \tag{15}$$

for the a_0 resonance and

$$F^{f_0}_S(\omega) = \frac{m^2_{f_0}}{m^2_{f_0} - \omega^2 - im_{f_0}(g_{\pi\pi}\rho_{\pi\pi} + g_{KK}\rho_{KK}F^2_{KK})}, \tag{16}$$

for the f_0 resonance [24,38,39]. In the case of the timelike form factor of the a_0 resonance, $C_{a_0} = |C_{a_0}|e^{i\phi_{a_0}}$ is the complex amplitude of the intermediate state a_0, with different values for the final states $\pi\eta$ and $K\bar{K}$. For the $K\bar{K}$ channel, the magnitude $|C^{KK}_{a_0}| = 1.07$ and phase $\phi_{a_0} = 82°$ [40]. Then, the phase of the $\pi\eta$ system is consistent with that of the $K\bar{K}$ system, and the module of the magnitude satisfies the relation $C^{\pi\eta}_{a_0}/C^{KK}_{a_0} = g_{a_0\pi\eta}/g_{a_0KK}$ according to the discussions in Ref. [21]. The definition of the strong coupling constants $g_{a_0KK}(g_{a_0\pi\eta})$ can be found in the literature [22,41]. In this article, we take the coupling constants as $g_{\pi\eta} = 0.324$ GeV and $g^2_{KK}/g^2_{\pi\eta} = 1.03$ through the Crystal Barrel experiment [42]. The values of the constants g_{a_0KK} and $g_{a_0\pi\eta}$ can be got with the relation $g_{KK}(g_{\eta\eta}) = g_{a_0KK}(g_{a_0\pi\eta})/(4\sqrt{\pi})$. Meanwhile, we employ the coupling constants $g_{\pi\pi} = 0.165 \pm 0.018$ GeV and $g_{KK}/g_{\pi\pi} = 4.21 \pm 0.33$ for f_0 [36], and introduce the factor $F_{KK} = e^{-\alpha q^2}$ into the timelike form factor $F^{f_0}_S(\omega)$ to suppress the $K\bar{K}$ contribution with the parameter $\alpha = 2.0 \pm 1.0$ GeV^{-2} [43]. In addition, the ρ factors are chosen as

$$\rho_{\pi\eta} = \sqrt{\left[1 - \left(\frac{m_\eta - m_\pi}{\omega}\right)^2\right]\left[1 - \left(\frac{m_\eta + m_\pi}{\omega}\right)^2\right]}, \tag{17}$$

$$\rho_{\pi\pi} = \frac{2}{3}\sqrt{1 - \frac{4m^2_{\pi^\pm}}{\omega^2}} + \frac{1}{3}\sqrt{1 - \frac{4m^2_{\pi^0}}{\omega^2}}, \tag{18}$$

$$\rho_{KK} = \frac{1}{2}\sqrt{1 - \frac{4m^2_{K^\pm}}{\omega^2}} + \frac{1}{2}\sqrt{1 - \frac{4m^2_{K^0}}{\omega^2}}. \tag{19}$$

The shape of the σ resonance can be well described by the Breit-Wigner model because it is a narrow intermediate resonance [44,45]:

$$F^\sigma_S(\omega) = \frac{C_\sigma m^2_\sigma}{m^2_\sigma - \omega^2 - im_\sigma\Gamma(\omega)}, \tag{20}$$

with the factor $C_\sigma = 3.50$ [43]. The energy-dependent width $\Gamma(\omega)$ in the case of a scalar resonance decaying into a pion pair can be parametrized as [33]

$$\Gamma(\omega) = \Gamma_0\frac{m_\sigma}{\omega}\left(\frac{\omega^2 - 4m^2_\pi}{m^2_\sigma - 4m^2_\pi}\right)^{\frac{1}{2}}, \tag{21}$$

where $\Gamma_0 = 0.40$ GeV is the width of the resonance.

In this paper, we take the mixing relation for the $f_0 - \sigma$ system [46],

$$\begin{pmatrix} \sigma \\ f_0 \end{pmatrix} = \begin{pmatrix} \cos\theta & -\sin\theta \\ \sin\theta & \cos\theta \end{pmatrix} \begin{pmatrix} f_n \\ f_s \end{pmatrix} \tag{22}$$

with

$$f_n = \frac{1}{\sqrt{2}}(u\bar{u} + d\bar{d}), \qquad f_s = s\bar{s}. \tag{23}$$

B. Helicity amplitudes

The $\bar{B}_s^0 \to a_0[\to \pi^0\eta, K\bar{K}]a_0$ decays only have annihilation Feynman diagrams, and their helicity amplitudes are written as

$$\mathcal{A}(\bar{B}_s^0 \to a_0^+[\to \pi^+\eta, K^+\bar{K}^0]a_0^-) = \frac{G_F}{\sqrt{2}} V_{ub}V_{us}^* \left[\left(C_1 + \frac{1}{3}C_2\right) F_e'^{LL} + C_2(M_g'^{LL}) \right]$$
$$- V_{tb}V_{ts}^* \left[(a_3 + a_5 + a_7 + a_9)F_e'^{LL} + \left(a_3 + a_5 - \frac{1}{2}(a_7 + a_9)\right)F_e^{LL} \right.$$
$$\left. + \left(C_4 - \frac{1}{2}C_{10}\right)M_g^{LL} + (C_4 + C_{10})M_g'^{LL} + \left(C_6 - \frac{1}{2}C_8\right)M_g^{SP} + (C_6 + C_8)M_g'^{SP} \right], \quad (24)$$

$$\mathcal{A}(\bar{B}_s^0 \to a_0^-[\to \pi^-\eta, K^-\bar{K}^0]a_0^+) = \frac{G_F}{\sqrt{2}} V_{ub}V_{us}^* \left[\left(C_1 + \frac{1}{3}C_2\right) F_e^{LL} + C_2(M_g^{LL}) \right] - V_{tb}V_{ts}^* \left[\left(a_3 + a_5 - \frac{1}{2}(a_7 + a_9)\right)F_e'^{LL} \right.$$
$$+ (a_3 + a_5 + a_7 + a_9)F_e^{LL} + (C_4 + C_{10})M_g^{LL} + \left(C_4 - \frac{1}{2}C_{10}\right)M_g'^{LL}$$
$$\left. + (C_6 + C_8)M_g^{SP} + \left(C_6 - \frac{1}{2}C_8\right)M_g'^{SP} \right], \tag{25}$$

$$\mathcal{A}(\bar{B}_s^0 \to a_0^0[\to \pi^0\eta, K^+K^-]a_0^0) = \frac{G_F}{2} V_{ub}V_{us}^* \left[\left(C_1 + \frac{1}{3}C_2\right)(F_e^{LL} + F_e'^{LL}) + C_2(M_g^{LL} + M_g'^{LL}) \right]$$
$$- V_{tb}V_{ts}^* \left[\left(2(a_3 + a_5) + \frac{1}{2}(a_7 + a_9)\right)(F_e^{LL} + F_e'^{LL}) + \left(2C_4 + \frac{1}{2}C_{10}\right)(M_g^{LL} + M_g'^{LL}) \right.$$
$$\left. + \left(2C_6 + \frac{1}{2}C_8\right)(M_g^{SP} + M_g'^{SP}) \right], \tag{26}$$

where $F_e(F_e')$ stands for the contributions of the factorizable annihilation diagrams shown in Figs. 1(e1), 1(f1), 1(e2), 1(f2), and $M_g(M_g')$ comes from the nonfactorizable annihilation diagrams in Figs. 1(g1), 1(h1), 1(g2), and 1(h2). In subsequent calculation, the function $F_a(F_a')$ denotes the contributions of the factorizable emission diagrams in Figs. 1(a1), 1(b1), 1(a2), 1(b2), and $M_c(M_c')$ comes from the nonfactorizable emission diagrams in Figs. 1(c1), 1(d1), 1(c2), and 1(d2). The specific expressions for the aforementioned functions are presented in the Appendix. The superscripts LL, LR, and SP represent the contributions of $(V-A)(V-A)$, $(V-A)(V+A)$, and $(S-P)(S+P)$ vertices, respectively.

Based on the $f_0 - \sigma$ mixing scheme, the helicity amplitudes of the $\bar{B}_s^0 \to f_0[\to \pi^+\pi^-, K^+K^-]f_0$, and $\bar{B}_s^0 \to \sigma[\to \pi^+\pi^-]\sigma$ decays are given by

$$\mathcal{A}(\bar{B}_s^0 \to f_0[\to \pi^+\pi^-, K^+K^-]f_0) = \sin^2\theta \mathcal{A}(\bar{B}_s^0 \to f_n[\to \pi^+\pi^-, K^+K^-]f_n) + \frac{1}{2}\sin 2\theta \mathcal{A}(\bar{B}_s^0 \to f_s[\to \pi^+\pi^-, K^+K^-]f_n)$$
$$+ \frac{1}{2}\sin 2\theta \mathcal{A}(\bar{B}_s^0 \to f_n[\to \pi^+\pi^-, K^+K^-]f_s) + \cos^2\theta \mathcal{A}(\bar{B}_s^0 \to f_s[\to \pi^+\pi^-, K^+K^-]f_s), \tag{27}$$

$$\mathcal{A}(\bar{B}_s^0 \to \sigma[\to \pi^+\pi^-]\sigma) = \cos^2\theta \mathcal{A}(\bar{B}_s^0 \to f_n[\to \pi^+\pi^-]f_n) - \frac{1}{2}\sin 2\theta \mathcal{A}(\bar{B}_s^0 \to f_s[\to \pi^+\pi^-]f_n)$$
$$- \frac{1}{2}\sin 2\theta \mathcal{A}(\bar{B}_s^0 \to f_n[\to \pi^+\pi^-]f_s) + \sin^2\theta \mathcal{A}(\bar{B}_s^0 \to f_s[\to \pi^+\pi^-]f_s), \tag{28}$$

with

$$\mathcal{A}(\bar{B}_s^0 \to f_s[\to \pi^+\pi^-, K^+K^-]f_s) = -G_F V_{tb} V_{ts}^* \left[\left(a_6 - \frac{1}{2} a_8 \right) (F_a^{SP} + F_e^{SP} + F_a'^{SP} + F_e'^{SP}) \right.$$

$$+ \left(a_3 + a_4 + a_5 - \frac{1}{2}(a_7 + a_9 + a_{10}) \right) (F_e^{LL} + F_e'^{LL})$$

$$+ \left(C_3 + C_4 - \frac{1}{2}(C_9 + C_{10}) \right) (M_c^{LL} + M_g^{LL} + M_c'^{LL} + M_g'^{LL})$$

$$+ \left(C_5 - \frac{1}{2} C_7 \right) (M_c^{LR} + M_g^{LR} + M_c'^{LR} + M_g'^{LR})$$

$$\left. + \left(C_6 - \frac{1}{2} C_8 \right) (M_c^{SP} + M_g^{SP} + M_c'^{SP} + M_g'^{SP}) \right], \tag{29}$$

$$\mathcal{A}(\bar{B}_s^0 \to f_s[\to \pi^+\pi^-, K^+K^-]f_n) = \frac{G_F}{2} \left[V_{ub} V_{us}^* C_2 M_c^{LL} - V_{tb} V_{ts}^* \left(\left(2C_4 + \frac{1}{2} C_{10} \right) M_c^{LL} + \left(2C_6 + \frac{1}{2} C_8 \right) M_c^{SP} \right) \right]. \tag{30}$$

Equation (30) is also applicable for $\bar{B}_s^0 \to f_n[\to \pi^+\pi^-, K^+K^-]f_s$ decay after replacing $M_c^{LL,SP}$ with $M_c'^{LL,'SP}$. Meanwhile, $\bar{B}_s^0 \to f_n[\to \pi^+\pi^-, K^+K^-]f_n$ decay has the same amplitude as $\bar{B}_s^0 \to a_0^0[\to \pi^0\eta, K^+K^-]a_0^0$ decay.

III. NUMERICAL RESULTS AND DISCUSSIONS

With the decay amplitudes $\mathcal{A}$, the differential branching ratio for the $\bar{B}_s^0 \to S[\to P_1P_2]S$ decays can be taken as

$$\frac{d\mathcal{B}}{d\omega} = \frac{\tau \omega |\vec{p}_1||\vec{p}_3|}{32\pi^3 M_B^3} |\bar{\mathcal{A}}|^2, \tag{31}$$

where τ is the B meson lifetime, $|\vec{p}_1|$ and $|\vec{p}_3|$, respectively, denote the magnitudes of momentum for one of the P_1P_2 meson pairs and the scalar meson S:

$$|\vec{p}_1| = \frac{\lambda^{1/2}(\omega^2, m_{P_1}^2, m_{P_2}^2)}{2\omega},$$

$$|\vec{p}_3| = \frac{\lambda^{1/2}(M_B^2, m_s^2, \omega^2)}{2\omega}, \tag{32}$$

with the Källén function $\lambda(a,b,c) = a^2 + b^2 + c^2 - 2(ab + ac + bc)$.

In Table I, we present the input parameters used in the calculations, including the masses of the mesons, the decay

constant and lifetime of the B_s^0 meson, and the Wolfenstein parameters of the CKM matrix elements [2,47,48].

By using the helicity amplitudes and the input parameters, we predict the CP-averaged branching fractions of the $\bar{B}_s^0 \to S[\to P_1P_2]S$ decays in the pQCD approach, and make some comments on the results. In Table II, we present the branching fractions of the $\bar{B}_s^0 \to a_0[\to \pi\eta, K\bar{K}]a_0$ decays. There are still many uncertainties in our calculation results. As shown in Table II, we primarily consider four types of errors, namely, the shape parameter of B meson $\omega_b = 0.50 \pm 0.05$ GeV, the Gegenbauer moment $a_2 = 0.3 \pm 0.1$ for the $K\bar{K}(\pi\eta)$ pair, the Gegenbauer moments $B_1 = -0.93 \pm 0.10$ and $B_3 = 0.14 \pm 0.08$ for the scalar meson a_0, and the scalar decay constant $\bar{f}_{a_0} = 0.365 \pm 0.020$ GeV. We have neglected the uncertainties caused by the mass of a_0 and the Wolfenstein parameters λ, A, ρ, η because they are typically very small. We notice that the main uncertainties come from the Gegenbauer moment in the wave function of the $K\bar{K}(\pi\eta)$ pair, thus, we look forward to obtaining more accurate experimental data in the future to reduce such errors.

Meanwhile, we can find the branching ratios of the $\bar{B}_s^0 \to a_0[\to \pi\eta]a_0$ decays are much larger than that of the $\bar{B}_s^0 \to a_0[\to K\bar{K}]a_0$ decays, which can be explained by the fact that the phase space for $K\bar{K}$ is suppressed. In the Ref. [22], the authors has predicted the branching ratios of the $B_s^0 \to a_0[\to \pi\eta, K\bar{K}]h$ (h denote the pseudoscalar meson π or K)

TABLE I. Input parameters of the $\bar{B}_s^0 \to S[\to P_1P_2]S$ decays.

$M_B = 5.367$ GeV	$m_b = 4.2$ GeV	$f_B = 227.2 \pm 3.4$ MeV	$\tau = 1.509$ ps
$m_{a_0} = 0.98 \pm 0.02$ GeV	$m_{f_0} = 0.99 \pm 0.02$ GeV	$m_\sigma = 0.5$ GeV	$m_{f_n} = 0.99$ GeV
$m_{f_s} = 1.02$ GeV	$m_{f_0(1500)} = 1.50$ GeV	$m_{\pi^\pm} = 0.14$ GeV	$m_{\pi^0} = 0.135$ GeV
$m_{K^\pm} = 0.494$ GeV	$m_{K^0} = 0.498$ GeV	$m_\eta = 0.548$ GeV	
$\lambda = 0.22453 \pm 0.00044$	$A = 0.836 \pm 0.015$	$\bar{\rho} = 0.122^{+0.018}_{-0.017}$	$\bar{\eta} = 0.355^{+0.012}_{-0.011}$

TABLE II. Branching ratios for the $\bar{B}_s^0 \to a_0[\to \pi\eta, K\bar{K}]a_0$ decays in the pQCD approach.

Decay modes	$\mathcal{B}$
$\bar{B}_s^0 \to a_0^0[\to \pi^0\eta]a_0^0$	$8.31^{+3.42}_{-2.26}(\omega_b)^{+6.06}_{-4.35}(a_2)^{+1.84}_{-0.61}(B)^{+0.93}_{-0.87}(\bar{f}_{a_0}) \times 10^{-8}$
$\bar{B}_s^0 \to a_0^0[\to K^+K^-]a_0^0$	$9.87^{+3.84}_{-2.61}(\omega_b)^{+6.76}_{-4.89}(a_2)^{+2.92}_{-1.34}(B)^{+1.07}_{-1.05}(\bar{f}_{a_0}) \times 10^{-9}$
$\bar{B}_s^0 \to a_0^+[\to \pi^+\eta]a_0^-$	$8.58^{+4.62}_{-3.35}(\omega_b)^{+5.33}_{-4.05}(a_2)^{+1.01}_{-0.93}(B)^{+0.97}_{-0.91}(\bar{f}_{a_0}) \times 10^{-7}$
$\bar{B}_s^0 \to a_0^+[\to K^+\bar{K}^0]a_0^-$	$1.76^{+0.95}_{-0.69}(\omega_b)^{+1.06}_{-0.81}(a_2)^{+0.20}_{-0.18}(B)^{+0.19}_{-0.18}(\bar{f}_{a_0}) \times 10^{-7}$
$\bar{B}_s^0 \to a_0^-[\to \pi^-\eta]a_0^+$	$8.76^{+4.66}_{-3.39}(\omega_b)^{+5.32}_{-4.06}(a_2)^{+1.11}_{-1.02}(B)^{+0.98}_{-0.93}(\bar{f}_{a_0}) \times 10^{-7}$
$\bar{B}_s^0 \to a_0^-[\to K^-K^0]a_0^+$	$1.81^{+0.98}_{-0.70}(\omega_b)^{+1.06}_{-0.82}(a_2)^{+0.23}_{-0.18}(B)^{+0.20}_{-0.19}(\bar{f}_{a_0}) \times 10^{-7}$

decays in the pQCD approach and get the results as follows: $\mathcal{B}(B_s^0 \to a_0^0[\to K^-K^+]\pi^0) = 0.04^{+0.00+0.01}_{-0.01-0.01} \times 10^{-6}$, $\mathcal{B}(B_s^0 \to a_0^0[\to \pi^0\eta]\pi^0) = 0.54^{+0.03+0.18}_{-0.05-0.10} \times 10^{-6}$; these are comparable to our results because these decay modes have the same components in the quark model and only annihilation contributions. The branching ratio of $\bar{B}_s^0 \to a_0^0[\to \pi^0\eta]a_0^0$ decay is much smaller than that of the $B_s^0 \to a_0^0[\to \pi^0\eta]\pi^0$ decay obviously, and the branching ratios of $\bar{B}_s^0 \to a_0^0[\to K^+K^-]a_0^0$ decay and $B_s^0 \to a_0^0[\to K^-K^+]\pi^0$ decay exhibit the same relationship, the reason may be that the QCD dynamics of the final state mesons a_0 and π^0 are different. At the same time, the authors also concluded that the branching fractions of the $\pi\eta$ channel was 5 times larger than that of the $K\bar{K}$ channel with the resonance $a_0(980)$ in Ref. [22]. Next, we will use our calculations to investigate the value of $\Gamma(a_0 \to K^+K^-)/\Gamma(a_0 \to \pi^0\eta)$ with the narrow-width approximation.

When the narrow-width approximation is considered, the branching ratio of the quasi-two-body decay can be written as

$$\mathcal{B}(B \to M_1(R \to)M_2M_3) \simeq \mathcal{B}(B \to M_1R) \times \mathcal{B}(R \to M_2M_3), \tag{33}$$

with the resonance R. We can define a ratio $\mathcal{R}_1$ as

$$\begin{aligned}
\mathcal{R}_1 &= \frac{\Gamma(a_0 \to K^+K^-)}{\Gamma(a_0 \to \pi^0\eta)} \\
&= \frac{\mathcal{B}(\bar{B}_s^0 \to a_0^0a_0^0) \times \mathcal{B}(a_0^0 \to K^+K^-)}{\mathcal{B}(\bar{B}_s^0 \to a_0^0a_0^0) \times \mathcal{B}(a_0^0 \to \pi^0\eta)} \\
&\simeq \frac{\mathcal{B}(\bar{B}_s^0 \to a_0^0[\to K^+K^-]a_0^0)}{\mathcal{B}(\bar{B}_s^0 \to a_0^0[\to \pi^0\eta]a_0^0)} \approx 0.12. \tag{34}
\end{aligned}$$

After considering the isospin relation $\Gamma(a_0 \to K^+K^-) = \Gamma(a_0 \to K\bar{K})/2$, we obtain the relative partial decay width $\Gamma(a_0 \to K\bar{K})/\Gamma(a_0 \to \pi\eta) \approx 0.24$. The OBELIX Collaboration acquired $\Gamma(a_0 \to K\bar{K})/\Gamma(a_0 \to \pi^0\eta) = 0.57 \pm 0.16$ through the coupled channel analysis of $\pi^+\pi^-\pi^0$, $K^+K^-\pi^0$ and $K^\pm K_S^0\pi^\mp$ [49]. In Ref. [42], the authors calculated the branching ratio of the $p\bar{p} \to$

$a_0(980)\pi \to K\bar{K}\pi$ decay $((5.92^{+0.46}_{-1.01}) \times 10^{-4})$, and combined with the data $\mathcal{B}(p\bar{p} \to a_0(980)\pi; a_0 \to \pi\eta) = (2.61 \pm 0.48) \times 10^{-3}$ in the annihilation channel $\pi^0\pi^0\eta$ [50], the ratio of the partial widths was determined as $\Gamma(a_0 \to K\bar{K})/\Gamma(a_0 \to \pi\eta) = 0.23 \pm 0.05$. The WA102 Collaboration gained $\Gamma(a_0 \to K\bar{K})/\Gamma(a_0 \to \pi\eta) = 0.166 \pm 0.01 \pm 0.02$ from the decay of $f_1(1285)$ [51]. The average relative partial decay widths is $\Gamma(a_0 \to K\bar{K})/\Gamma(a_0 \to \pi\eta) = 0.183 \pm 0.024$ given by the Particle Data Group [2]. It is obvious that our results are slightly larger than the average ratio, but are in agreement with the data in Ref. [42] within errors.

For the $\bar{B}_s^0 \to f_0[\to \pi^+\pi^-, K^+K^-]f_0$ and $\bar{B}_s^0 \to \sigma[\to \pi^+\pi^-]\sigma$ decays, the scalars f_0 and σ are not only regarded as $s\bar{s}$, but also contain $(u\bar{u} + d\bar{d})/\sqrt{2}$ in the quark model. The mixing angle θ is introduced into the $f_0 - \sigma$ mixing mechanism. In this case, the decay amplitudes of the $\bar{B}_s^0 \to f_0[\to \pi^+\pi^-, K^+K^-]f_0$ and $\bar{B}_s^0 \to \sigma[\to \pi^+\pi^-]\sigma$ decays consist of four parts, and the total amplitudes are related to these four parts by the mixing angle θ, which can be found in Eqs. (27) and (28). We then plot the branching fractions of $\bar{B}_s^0 \to f_0[\to \pi^+\pi^-]f_0$ and $\bar{B}_s^0 \to \sigma[\to \pi^+\pi^-]\sigma$ decays dependent on the free parameter θ in Fig. 2. The branching ratio of the $\bar{B}_s^0 \to f_0[\to \pi^+\pi^-]f_0$ decay obeys the cos law, as can be seen in Fig. 2(a), while the other channel's contribution satisfies the sin law, as can be seen in Fig. 2(b). Considering both decays, the range of the mixing angle θ can be set as [15°, 82°] and [105°, 171°] because the branching ratios of both decays are close to zero when θ takes other values. This range is larger than that of the two-body decays $\bar{B}_s^0 \to f_0f_0$ and $\bar{B}_s^0 \to \sigma\sigma$, but still consistent with the data in the Refs. [46,52,53].

The mixing angle θ is not fixed for the $f_0 - \sigma$ system, and the value may vary in different works depending on the study requirements [24,54,55]. In the current study, we take $\theta = 30°$ to make numerical calculations, and this value also satisfies the results presented by the LHCb Collaboration [45]. Taking the mixing angle into account, the averaged branching ratios for the $\bar{B}_s^0 \to f_0[\to \pi^+\pi^-, K^+K^-]f_0$ and $\bar{B}_s^0 \to \sigma[\to \pi^+\pi^-]\sigma$ decays are presented in Table III.

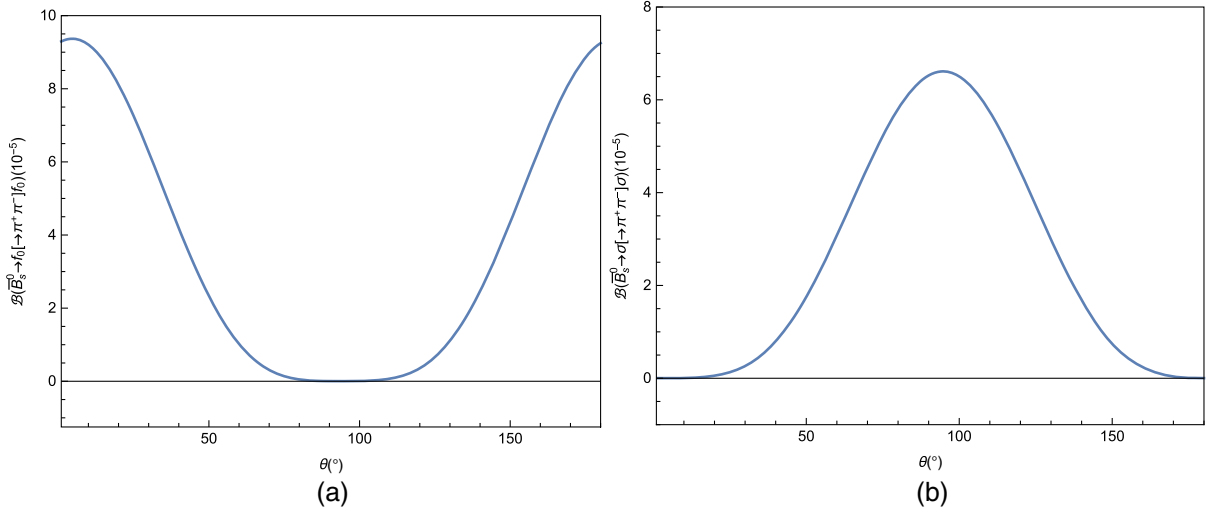As can be seen in Table III, the major uncertainties originate from the shape parameter ω_b of the B meson's

FIG. 2. (a) The branching ratio of $\bar{B}_s^0 \to f_0[\to \pi^+\pi^-]f_0$ decay on the mixing angle θ; (b) the branching ratio of $\bar{B}_s^0 \to \sigma[\to \pi^+\pi^-]\sigma$ decay on the mixing angle θ.

wave function for both $\bar{B}_s^0 \to f_0[\to \pi^+\pi^-, K^+K^-]f_0$ and $\bar{B}_s^0 \to \sigma[\to \pi^+\pi^-]\sigma$ decays. We still can find the branching ratio for the $\bar{B}_s^0 \to f_0[\to \pi^+\pi^-]f_0$ decay is larger than that of the $\bar{B}_s^0 \to \sigma[\to \pi^+\pi^-]\sigma$ decay by 1 order of magnitude, we think the reason for this result may be that the scalar meson f_0 has a greater mass than σ. When we take the mixing angle $\theta = 0°$, f_0 is regarded as the pure $s\bar{s}$, and the branching ratio of $\bar{B}_s^0 \to f_0[\to \pi^+\pi^-]f_0$ is about 9.29×10^{-5}. Whereas for $\bar{B}_s^0 \to \sigma[\to \pi^+\pi^-]\sigma$ decay, the branching ratio is very small with $\theta = 0°$, and the value will increase a lot after considering the mixing of $s\bar{s}$. Therefore, $\bar{B}_s^0 \to f_s[\to \pi^+\pi^-, K^+K^-]f_s$ makes the dominant contribution in the branching ratios. Numerical results of $\bar{B}_s^0 \to f_0[\to \pi^0\pi^0]f_0$ and $\bar{B}_s^0 \to \sigma[\to \pi^0\pi^0]\sigma$ decays are obtained with the isospin relationship $\mathcal{B}(f_0(\sigma) \to \pi^+\pi^-)/\mathcal{B}(f_0(\sigma) \to \pi^0\pi^0) = 2$. The magnitudes of the predicted branching ratios are at the order of $10^{-5} \sim 10^{-6}$, we expect these results can be tested by the LHCb and Belle II experiments in the near future.

To compare with existing data and further discuss our calculations, we then use the narrow-width approximation to study the $\bar{B}_s^0 \to f_0[\to \pi^+\pi^-, K^+K^-]f_0$ decays. The $\bar{B}_s^0 \to f_0[\to \pi^+\pi^-]f_0$ and $\bar{B}_s^0 \to f_0[\to K^+K^-]f_0$ decays

have the same resonance, we can define a ratio $\mathcal{R}_2$ to describe the relationship between $f_0 \to \pi^+\pi^-$ and $f_0 \to K^+K^-$, which can be given as

$$
\begin{aligned}
\mathcal{R}_2 &= \frac{\mathcal{B}(f_0 \to K^+K^-)}{\mathcal{B}(f_0 \to \pi^+\pi^-)} \\
&= \frac{\mathcal{B}(\bar{B}_s^0 \to f_0 f_0) \times \mathcal{B}(f_0 \to K^+K^-)}{\mathcal{B}(\bar{B}_s^0 \to f_0 f_0) \times \mathcal{B}(f_0 \to \pi^+\pi^-)} \\
&\simeq \frac{\mathcal{B}(\bar{B}_s^0 \to f_0[\to K^+K^-]f_0)}{\mathcal{B}(\bar{B}_s^0 \to f_0[\to \pi^+\pi^-]f_0)} \approx 0.17,
\end{aligned}
\tag{35}
$$

this ratio can be used to estimate the branching ratios for the $f_0 \to \pi^+\pi^-$ and $f_0 \to K^+K^-$ decays by using the formulas $\mathcal{B}(f_0 \to \pi^+\pi^-) = \frac{2}{4\mathcal{R}_2+3}$ and $\mathcal{B}(f_0 \to K^+K^-) = \frac{2\mathcal{R}_2}{4\mathcal{R}_2+3}$ [56]. So we can get

$$
\mathcal{B}(f_0 \to \pi^+\pi^-) \approx 0.54,
$$
$$
\mathcal{B}(f_0 \to K^+K^-) \approx 0.09.
\tag{36}
$$

The BES Collaboration gained the relative branching ratios through the $\psi(2S) \to \gamma\chi_{c0}$ decays, where $\chi_{c0} \to f_0 f_0 \to \pi^+\pi^-\pi^+\pi^-$ or $\chi_{c0} \to f_0 f_0 \to \pi^+\pi^- K^+K^-$ [57,58].
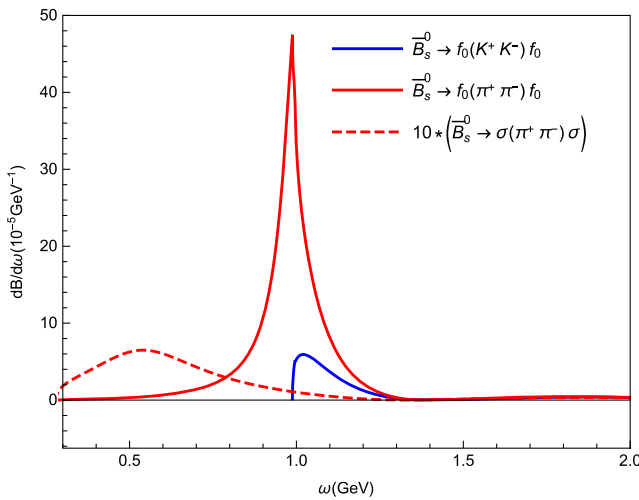
TABLE III. Branching ratios for the $\bar{B}_s^0 \to f_0[\to \pi^+\pi^-, K^+K^-]f_0$ and $\bar{B}_s^0 \to \sigma[\to \pi^+\pi^-]\sigma$ decays in the pQCD approach with the $f_0 - \sigma$ mixing angle $\theta = 30°$.

Decay modes	$\theta = 30°$
$\bar{B}_s^0 \to f_0[\to \pi^+\pi^-]f_0$	$6.07^{+2.04}_{-1.69}(\omega_b)^{+0.91}_{-0.83}(a_2)^{+0.70}_{-0.63}(B)^{+0.67}_{-0.64}(\bar{f}_s) \times 10^{-5}$
$\bar{B}_s^0 \to f_0[\to K^+K^-]f_0$	$1.02^{+0.36}_{-0.29}(\omega_b)^{+0.13}_{-0.12}(a_2)^{+0.11}_{-0.09}(B)^{+0.11}_{-0.10}(\bar{f}_s) \times 10^{-5}$
$\bar{B}_s^0 \to f_0[\to \pi^0\pi^0]f_0$	$3.03^{+1.02}_{-0.85}(\omega_b)^{+0.45}_{-0.41}(a_2)^{+0.35}_{-0.31}(B)^{+0.34}_{-0.32}(\bar{f}_s) \times 10^{-5}$
$\bar{B}_s^0 \to \sigma[\to \pi^+\pi^-]\sigma$	$3.01^{+0.85}_{-0.72}(\omega_b)^{+0.36}_{-0.20}(a_2)^{+0.09}_{-0.05}(B)^{+0.33}_{-0.31}(\bar{f}_s) \times 10^{-6}$
$\bar{B}_s^0 \to \sigma[\to \pi^0\pi^0]\sigma$	$1.50^{+0.42}_{-0.36}(\omega_b)^{+0.18}_{-0.10}(a_2)^{+0.05}_{-0.02}(B)^{+0.17}_{-0.16}(\bar{f}_s) \times 10^{-6}$
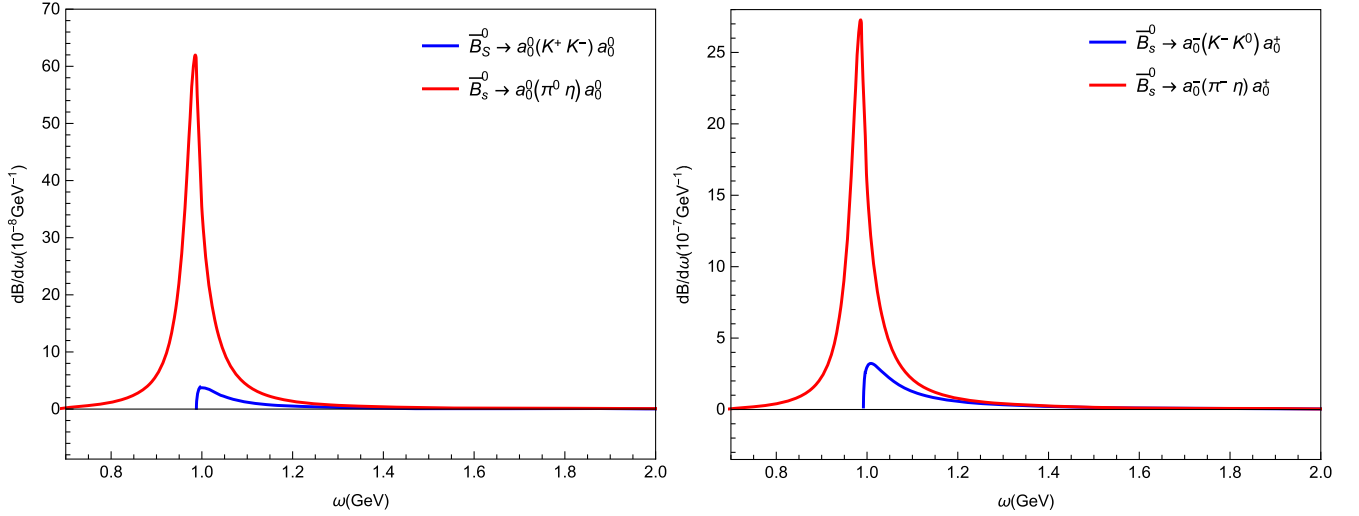
FIG. 3.   Differential branching fractions of the $\bar{B}_s^0 \to a_0[\to K\bar{K}, \pi\eta]a_0$ decays.

Meanwhile, the CLEO Collaboration has obtained $\mathcal{B}(f_0 \to K^+K^-)/\mathcal{B}(f_0 \to \pi^+\pi^-) = (25^{+17}_{-11})\%$ and extracted $\mathcal{B}(f_0 \to \pi^+\pi^-) = (50^{+7}_{-9})\%$ by using the results of BES Collaboration [59], and our calculations are still consistent with that in CLEO Collaboration.

In Fig. 3, we graph the differential branching ratios of the $\bar{B}_s^0 \to a_0[\to K\bar{K}, \pi\eta]a_0$ decays on the invariant mass, the results of $\bar{B}_s^0 \to a_0^0[\to K^+K^-, \pi^0\eta]a_0^0$ models are shown on the left and those of $\bar{B}_s^0 \to a_0^-[\to K^-K^0, \pi^-\eta]a_0^+$ models are shown on the right. The differential branching ratios of $\bar{B}_s^0 \to f_0[\to \pi^+\pi^-]f_0$, $\bar{B}_s^0 \to f_0[\to K^+K^-]f_0$, and $\bar{B}_s^0 \to \sigma[\to \pi^+\pi^-]\sigma$ decays on the $\pi\pi$ or $K\bar{K}$ invariant mass ω are presented in Fig. 4 with red solid line, blue solid line, and red dashed line, respectively. For the a_0 resonance, the contributions of the $K\bar{K}$ channel are much smaller than that

of the $\pi\eta$ channel, and for the $d\mathcal{B}(\bar{B}_s^0 \to \sigma[\to \pi^+\pi^-]\sigma)/d\omega$ mode, we magnify the results tenfold for easy viewing. From the figures, it is clear that the peak occurs around the resonance peak mass, and the majority of the branching ratios are concentrated around the resonance state, basically in the range of $[m_S - \Gamma_S, m_S + \Gamma_S]$. Here, we do not plot the contributions of $\bar{B}_s^0 \to a_0^+[\to K^+\bar{K}^0, \pi^+\eta]a_0^-$ channels separately, because their results are very similar to the results of $\bar{B}_s^0 \to a_0^-[\to K^-K^0, \pi^-\eta]a_0^+$ channels.

IV. SUMMARY

In this article, we predict the branching fractions of $\bar{B}_s^0 \to a_0[\to K\bar{K}, \pi\eta]a_0$, $\bar{B}_s^0 \to f_0[\to \pi^+\pi^-, K^+K^-]f_0$ and $\bar{B}_s^0 \to \sigma[\to \pi^+\pi^-]\sigma$ decays with the pQCD approach first, where the scalars are considered as the $q\bar{q}$ state in the first scenario. Our results show that (i) For the $\bar{B}_s^0 \to a_0[\to K\bar{K}, \pi\eta]a_0$ decays, the largest branching ratio is $\mathcal{B}(\bar{B}_s^0 \to a_0^-[\to \pi^-\eta]a_0^+) = 8.76 \times 10^{-7}$, which is highly likely to be verified experimentally; (ii) For the $\bar{B}_s^0 \to f_0[\to \pi^+\pi^-, K^+K^-]f_0$ and $\bar{B}_s^0 \to \sigma[\to \pi^+\pi^-]\sigma$ decays, we consider that the scalars f_0 and σ contain $s\bar{s}$ and $(u\bar{u} + d\bar{d})/\sqrt{2}$ components in the quark model, so our calculations are carried out with the $f_0 - \sigma$ mixing scheme, when the value of the mixing angle θ is taken as $30°$, our results are at the order of 10^{-6}–10^{-5}. Using the narrow-width approximation, we calculate the relative partial decay widths $\Gamma(a_0 \to K\bar{K})/\Gamma(a_0 \to \pi\eta)$ and the ratio $\mathcal{B}(f_0 \to K^+K^-)/\mathcal{B}(f_0 \to \pi^+\pi^-)$, which are in agreement with the existing experimental values. Our work has positive implications for understanding the QCD behavior of the scalars, and we also expect that our calculations can be tested by the LHCb and Belle II experiments in the future.

FIG. 4.   Differential branching fractions of the $\bar{B}_s^0 \to f_0[\to \pi^+\pi^-, K^+K^-]f_0$ and $\bar{B}_s^0 \to \sigma[\to \pi^+\pi^-]\sigma$ decays.

ACKNOWLEDGMENTS

APPENDIX: FACTORIZATION FORMULAS

In this Appendix, we list the factorization formulas that are used in Eqs. (24)–(30). According to previous studies [38,60], we can find the formulas for the factorization diagrams related to the decays $B \to S[\to PP]V$. In

our work, the formulas for the factorization diagrams for the case when the final-state scalars are emitted are roughly consistent with those shown in Ref. [60]. In contrast, for the factorization diagrams where the PP meson pair is emitted or for the annihilation diagrams, the formulas are different from that in the existing works because of the difference in the wave functions between the final-state scalars and other mesons. So we recalculate the contributions of the Feynman diagrams. First, we give the contribution of the factorization diagrams in Figs. 1(a1) and 1(b1) with different currents, which are

(1) $(V-A)(V-A)$

$$
F_a^{LL} = -4\pi C_F f_s M_B^4 \int_0^1 dx_B dz \int_0^\infty b_B db_B b db \phi_B(x_B, b_B)
$$
$$
\times \left\{ [-2\bar{\eta}z\phi_S(z) + \sqrt{(1-r^2)}\eta\bar{\eta}(2r_b + r^2(z-2) - z)(\phi_S^s(z) - \phi_S^t(z)) \right.
$$
$$
+ 4\sqrt{(1-r^2)}\eta r_b r^2 \phi_S^t(z)]\alpha_s(t_{a1})h_{a1}(\alpha_{a1}, \beta_{a1}, b_B, b)\exp[-S_B(t_{a1}) - S(t_{a1})]S_t(z)
$$
$$
+ [2(r^2(x_B - \eta) - \eta\bar{\eta})\phi_S(z) - 4\sqrt{(1-r^2)}\eta\bar{\eta}\phi_S^s(z)]\alpha_s(t_{b1})h_{b1}(\alpha_{b1}, \beta_{b1}, b, b_B)
$$
$$
\left. \times \exp[-S_B(t_{b1}) - S(t_{b1})]S_t(|x_B - \eta|) \right\}. \tag{A1}
$$

(2) $(V-A)(V+A)$

$$
F_a^{LR} = F_a^{LL}. \tag{A2}
$$

(3) $(S-P)(S+P)$

$$
F_a^{SP} = 8\pi C_F \bar{f}_s M_B^4 r \int_0^1 dx_B dz \int_0^\infty b_B db_B b db \phi_B(x_B, b_B)
$$
$$
\times \left\{ [(2r_b(1-r^2+\eta) + 4(\eta\bar{z} - 1))\phi_S(z) - 2\sqrt{(1-r^2)}\eta(z+\bar{\eta})(\phi_S^s(z) - \phi_S^t(z)) - 4\sqrt{(1-r^2)}\eta \right.
$$
$$
\times (r^2\bar{z} + z)\phi_S^t(z) + 8\sqrt{(1-r^2)}\eta r_b \phi_S^s(z)]\alpha_s(t_{a1})h_{a1}(\alpha_{a1}, \beta_{a1}, b_B, b)\exp[-S_B(t_{a1}) - S(t_{a1})]S_t(z)
$$
$$
+ [2(r^2-1)(x_B - 2\eta)\phi_S(z) - 4\sqrt{(1-r^2)}\eta(r^2 - \bar{x}_B - \eta)\phi_S^s(z)]
$$
$$
\left. \times \alpha_s(t_{b1})h_{b1}(\alpha_{b1}, \beta_{b1}, b, b_B)\exp[-S_B(t_{b1}) - S(t_{b1})]S_t(|x_B - \eta|) \right\}, \tag{A3}
$$

with $\bar{x}_i = 1 - x_i$, $\bar{\eta} = 1 - \eta$. $C_F = \frac{4}{3}$ stands for the color factor. We take $F_a^{LL} = F_a^{LR} = 0$ because of the vector decay constant's small value. And the nonfactorization diagrams in Figs. 1(c1) and 1(d1) give

(1) $(V-A)(V-A)$

$$
M_c^{LL} = \frac{4\pi C_F M_B^4}{\sqrt{2N_c}} \int_0^1 dx_B dz dx_3 \int_0^\infty b_B db_B b_3 db_3 \phi_B(x_B, b_B)\phi_S(x_3)
$$
$$
\times \left\{ [4\bar{\eta}(x_B + (z-2)\eta + x_3\bar{\eta})\phi_S(z) + 4\sqrt{(1-r^2)}\eta\bar{z}\bar{\eta}(\phi_S^s(z) - \phi_S^t(z)) - 8\sqrt{(1-r^2)}\eta\bar{z}\bar{\eta}\phi_S^t(z)] \right.
$$
$$
\times \alpha_s(t_{c1})h_{c1}(\alpha_{c1}, \beta_{c1}, b_3, b_B)\exp[-S_B(t_{c1}) - S(t_{c1}) - S_3(t_{c1})]
$$
$$
+ [\bar{\eta}(2 - x_B - z - x_3\bar{\eta})\phi_S(z) + 4\sqrt{(1-r^2)}\eta\bar{z}\bar{\eta}(\bar{x}_B + z\bar{\eta} - 2x_3\bar{\eta})(\phi_S^s(z) - \phi_S^t(z))
$$
$$
\left. + 8\sqrt{(1-r^2)}\eta r^2(\bar{x}_B - x_3\bar{\eta})\phi_S^t(z)]\alpha_s(t_{d1})h_{d1}(\alpha_{d1}, \beta_{d1}, b_3, b_B)\exp[-S_B(t_{d1}) - S(t_{d1}) - S_3(t_{d1})] \right\}. \tag{A4}
$$

(2) $(V-A)(V+A)$

$$
\begin{aligned}
M_c^{LR} = \frac{4\pi C_F M_B^4}{\sqrt{2N_c}} \int_0^1 dx_B dz dx_3 \int_0^\infty & b_B db_B b_3 db_3 \phi_B(x_B, b_B) \\
\times \Big\{ & \big[4\sqrt{(1-r^2)}\eta r(\bar{z} - x_B + \eta\bar{x}_3)(\phi_S^s(z) - \phi_S^t(z))(\phi_S^S(x_3) - \phi_S^T(x_3)) + 8\sqrt{(1-r^2)}\eta r\bar{z} \\
\times & \phi_S^T(x_3)(\phi_S^s(z) - \phi_S^t(z)) - 8\sqrt{(1-r^2)}\eta r(x_B - \eta - x_3\bar{\eta})\phi_S^t(z)(\phi_S^S(x_3) - \phi_S^T(x_3)) \\
- & 4r(-(x_B + \eta(z-2)) + x_3\bar{\eta})\phi_S(z)(\phi_S^S(x_3) - \phi_S^T(x_3)) - 8r\eta(\bar{z} + r^2(x_3 - \bar{z}))\phi_S(z)\phi_S^T(x_3)\big] \\
\times & \alpha_s(t_{c1})h_{c1}(\alpha_{c1}, \beta_{c1}, b_3, b_B) \exp[-S_B(t_{c1}) - S(t_{c1}) - S_3(t_{c1})] \\
+ & \big[4\sqrt{(1-r^2)}\eta r(-2 + x_B + z + x_3\bar{\eta})(\phi_S^s(z) - \phi_S^t(z))(\phi_S^S(x_3) - \phi_S^T(x_3)) + 8\sqrt{(1-r^2)}\eta r(\bar{x}_B - x_3\bar{\eta}) \\
\times & \phi_S^T(x_3)(\phi_S^s(z) - \phi_S^t(z)) - 4r(x_3\bar{\eta} - \bar{x}_B - \eta\bar{z})\phi_S(z)(\phi_S^S(x_3) - \phi_S^T(x_3)) + 4r(r^2 - 1)(x_3\bar{\eta} - \bar{x}_B)\phi_S(z)\phi_S^T(x_3)\big] \\
\times & \alpha_s(t_{d1})h_{d1}(\alpha_{d1}, \beta_{d1}, b_3, b_B) \exp[-S_B(t_{d1}) - S(t_{d1}) - S_3(t_{d1})] \Big\}.
\end{aligned}
\tag{A5}
$$

(3) $(S-P)(S+P)$

$$
\begin{aligned}
M_c^{SP} = \frac{-8\pi C_F M_B^4}{\sqrt{2N_c}} \int_0^1 dx_B dz dx_3 \int_0^\infty & b_B db_B b_3 db_3 \phi_B(x_B, b_B)\phi_S(x_3) \\
\times \Big\{ & \big[2\bar{\eta}(x_3 - x_B + \bar{z} + \eta\bar{x}_3)\phi_S(z) + 2\sqrt{(1-r^2)}\eta\bar{\eta}\,\bar{z}(\phi_S^s(z) - \phi_S^t(z)) \\
- & 4\sqrt{(1-r^2)}\eta r^2(x_B - \eta - x_3\bar{\eta})\phi_S^t(z)\big]\alpha_s(t_{c1})h_{c1}(\alpha_{c1}, \beta_{c1}, b_3, b_B) \exp[-S_B(t_{c1}) - S(t_{c1}) - S_3(t_{c1})] \\
+ & \big[2\bar{\eta}(\bar{\eta}x_3 - \eta\bar{z} - \bar{x}_B)\phi_S(z) - 2\sqrt{(1-r^2)}\eta\bar{\eta}\,\bar{z}(\phi_S^s(z) + \phi_S^t(z))\big] \\
\times & \alpha_s(t_{d1})h_{d1}(\alpha_{d1}, \beta_{d1}, b_3, b_B) \exp[-S_B(t_{d1}) - S(t_{d1}) - S_3(t_{d1})] \Big\}.
\end{aligned}
\tag{A6}
$$

The contributions of the factorizable annihilation diagrams in Figs. 1(e1) and 1(f1) are
(1) $(V-A)(V-A)$

$$
\begin{aligned}
F_e^{LL} = -2\pi C_F f_B M_B^4 \int_0^1 dz dx_3 \int_0^\infty & b db b_3 db_3 \big\{ \big[2\bar{\eta}(x_3\bar{\eta} - 1)\phi_S(z)\phi_S(x_3) - 4\sqrt{(1-r^2)}\eta r(-2 + x_3\bar{\eta})\phi_S^s(z)\phi_S^S(x_3) \\
+ & 4\sqrt{(1-r^2)}\eta r x_3\bar{\eta}\phi_S^s(z)\phi_S^T(x_3)\big]\alpha_s(t_{e1})h_{e1}(\alpha_{e1}, \beta_{e1}, b, b_3) \exp[-S_3(t_{e1}) - S(t_{e1})]S_t(x_3) \\
+ & \big[2z\bar{\eta}\phi_S(z)\phi_S(x_3) - 4\sqrt{(1-r^2)}\eta r^2 r(\bar{\eta} + z)\phi_S^s(z)\phi_S^S(x_3) + 4\sqrt{(1-r^2)}\eta r^2 r(\bar{\eta} - z)\phi_S^t(z)\phi_S^S(x_3)\big] \\
\times & \alpha_s(t_{f1})h_{f1}(\alpha_{f1}, \beta_{f1}, b_3, b) \exp[-S_3(t_{f1}) - S(t_{f1})]S_t(z) \big\}.
\end{aligned}
\tag{A7}
$$

(2) $(V-A)(V+A)$

$$
F_e^{LR} = F_e^{LL}.
\tag{A8}
$$

(3) $(S-P)(S+P)$

$$
\begin{aligned}
F_e^{SP} = -4\pi C_F f_B M_B^4 \int_0^1 dz dx_3 \int_0^\infty & b db b_3 db_3 \\
\times \Big\{ & \big[2r(x_3\bar{\eta} - 1 - \eta)\phi_S(z)(\phi_S^S(x_3) - \phi_S^T(x_3)) - 4r(1 - x_3\bar{\eta})\phi_S(z)\phi_S^T(x_3) + 4\sqrt{(1-r^2)}\eta\bar{\eta}\phi_S^s(z)\phi_S(x_3)\big] \\
\times & \alpha_s(t_{e1})h_{e1}(\alpha_{e1}, \beta_{e1}, b, b_3) \exp[-S_3(t_{e1}) - S(t_{e1})]S_t(x_3) \\
+ & \big[4r(\eta\bar{z} - 1)\phi_S(z)\phi_S^S(x_3) + 2\sqrt{(1-r^2)}\eta z\bar{\eta}\phi_S(x_3)(\phi_S^s(z) - \phi_S^t(z)) + 4\sqrt{(1-r^2)}\eta r^2\bar{\eta}\phi_S(x_3)\phi_S^t(z)\big] \\
\times & \alpha_s(t_{f1})h_{f1}(\alpha_{f1}, \beta_{f1}, b_3, b) \exp[-S_3(t_{f1}) - S(t_{f1})]S_t(z) \Big\}.
\end{aligned}
\tag{A9}
$$

The contributions of the nonfactorizable annihilation diagrams in Figs. 1(g1) and 1(h1) are

(1) $(V-A)(V-A)$

$$
\begin{aligned}
M_g^{LL} =& \frac{4\pi C_F M_B^4}{\sqrt{2N_c}} \int_0^1 dx_B dz dx_3 \int_0^\infty b_B db_B b_3 db_3 \phi_B(x_B, b_B) \\
& \times \{[4(1+\eta)z\bar{\eta}\phi_S(z)\phi_S(x_3) + 4\sqrt{(1-r^2)\eta}r(x_B - z - \bar{x}_3\bar{\eta})(\phi_S^s(z)\phi_S^S(x_3) - \phi_S^t(z)\phi_S^T(x_3)) + 4\sqrt{(1-r^2)\eta}r \\
& \times (x_B + z - \bar{x}_3\bar{\eta})(\phi_S(z)\phi_S^T(x_3) - \phi_S^t(z)\phi_S^S(x_3))]\alpha_s(t_{g1})h_{g1}(\alpha_{g1}, \beta_{g1}, b_B, b_3)\exp[-S_B(t_{g1}) - S(t_{g1}) - S_3(t_{g1})] \\
& + [4\bar{\eta}(x_3\bar{\eta} - (x_B + (z-2)\eta) + r_b)\phi_S(z)\phi_S(x_3) - 4\sqrt{(1-r^2)\eta}r(\bar{z} + x_3\bar{\eta} + \eta - x_B)(\phi_S^s(z)\phi_S^S(x_3) - \phi_S^t(z)\phi_S^T(x_3)) \\
& - 4\sqrt{(1-r^2)\eta}r(\bar{z} - x_3\bar{\eta} + x_B - \eta)(\phi_S(z)\phi_S^T(x_3) - \phi_S^t(z)\phi_S^S(x_3)) + 16\sqrt{(1-r^2)\eta}rr_b\phi_S^s(z)\phi_S^S(x_3)] \\
& \times \alpha_s(t_{g1})h_{g1}(\alpha_{h1}, \beta_{h1}, b_B, b_3)\exp[-S_B(t_{h1}) - S(t_{h1}) - S_3(t_{h1})]\}.
\end{aligned}
\tag{A10}
$$

(2) $(V-A)(V+A)$

$$
\begin{aligned}
M_g^{LR} =& \frac{-4\pi C_F M_B^4}{\sqrt{2N_c}} \int_0^1 dx_B dz dx_3 \int_0^\infty b_B db_B b_3 db_3 \phi_B(x_B, b_B) \\
& \times \{[-4r(x_3\bar{\eta} + \eta\bar{z} - \bar{x}_B)\phi_S(z)(\phi_S^S(x_3) - \phi_S^T(x_3)) + 8rz\eta\phi_S(z)\phi_S^T(x_3) + 4\sqrt{(1-r^2)\eta}(z\bar{\eta} + \eta\bar{z} + \eta) \\
& \times \phi_S(x_3)(\phi_S^s(z) - \phi_S^t(z)) + 8\sqrt{(1-r^2)\eta}z\bar{\eta}\phi_S(x_3)\phi_S^t(z)]\alpha_s(t_{g1})h_{g1}(\alpha_{g1}, \beta_{g1}, b_B, b_3) \\
& \times \exp[-S_B(t_{g1}) - S(t_{g1}) - S_3(t_{g1})] + [4r(x_3\bar{\eta} - x_B + \eta(2-z))\phi_S(z)(\phi_S^S(x_3) - \phi_S^T(x_3)) + 8r\eta\bar{z}\phi_S(z)\phi_S^T(x_3) \\
& + 4\sqrt{(1-r^2)\eta}\eta\bar{\eta}(\bar{z} + 1)\phi_S(x_3)(\phi_S^s(z) + \phi_S^t(z)) + 4rr_b(1+\eta)\phi_S(z)(\phi_S^S(x_3) - \phi_S^T(x_3)) + 8rr_b\eta\phi_S(z)\phi_S^T(x_3)] \\
& \times \alpha_s(t_{g1})h_{g1}(\alpha_{h1}, \beta_{h1}, b_B, b_3)\exp[-S_B(t_{h1}) - S(t_{h1}) - S_3(t_{h1})]\}.
\end{aligned}
\tag{A11}
$$

(3) $(S-P)(S+P)$

$$
\begin{aligned}
M_g^{SP} =& \frac{8\pi C_F M_B^4}{\sqrt{2N_c}} \int_0^1 dx_B dz dx_3 \int_0^\infty b_B db_B b_3 db_3 \phi_B(x_B, b_B) \\
& \times \{[2\bar{\eta}(\eta\bar{z} + x_3\bar{\eta} - \bar{x}_B)\phi_S(z)\phi_S(x_3) + 2\sqrt{(1-r^2)\eta}r(x_B - z - \bar{x}_3\bar{\eta})(\phi_S^t(z)\phi_S^T(x_3) - \phi_S^s(z)\phi_S^S(x_3)) \\
& + 2\sqrt{(1-r^2)\eta}r(x_B + z - \bar{x}_3\bar{\eta})(\phi_S^s(z)\phi_S^T(x_3) - \phi_S^t(z)\phi_S^S(x_3))]\alpha_s(t_{g1})h_{g1}(\alpha_{g1}, \beta_{g1}, b_B, b_3) \\
& \times \exp[-S_B(t_{g1}) - S(t_{g1}) - S_3(t_{g1})] + [2(-\bar{z}\bar{\eta}(1+\eta) + r_b\bar{\eta})\phi_S(z)\phi_S(x_3) - 2\sqrt{(1-r^2)\eta}r(\eta - x_B + x_3\bar{\eta} + \bar{z}) \\
& \times (\phi_S^t(z)\phi_S^T(x_3) - \phi_S^s(z)\phi_S^S(x_3)) - 2\sqrt{(1-r^2)\eta}r(x_B - \eta - x_3\bar{\eta} + \bar{z})(\phi_S^s(z)\phi_S^T(x_3) - \phi_S^t(z)\phi_S^S(x_3))] \\
& \times \alpha_s(t_{h1})h_{h1}(\alpha_{h1}, \beta_{h1}, b_B, b_3)\exp[-S_B(t_{h1}) - S(t_{h1}) - S_3(t_{h1})]\}.
\end{aligned}
\tag{A12}
$$

In Figs. 1(a2) and 1(b2), we can see the meson pair will be factorized out, when taking the $(V-A)(V-A)$ and $(V-A)(V+A)$ currents into account, the S-wave meson pair cannot be emitted because of the charge conjugation invariance, so

$$
F_a^{\prime LL} = F_a^{\prime LR} = 0
\tag{A13}
$$

$$F_a'^{SP} = 8\pi C_F \bar{f}_s \sqrt{\eta} M_B^4 r \int_0^1 dx_B dx_3 \int_0^\infty b_B db_B b_3 db_3 \phi_B(x_B, b_B)$$
$$\times \{[2\bar{\eta}(r_b - 2)\phi_S(x_3) - 2r(1 + \eta + x_3\bar{\eta})(\phi_S^S(x_3) - \phi_S^T(x_3)) - 4r\phi_S^T(x_3) + 8rr_b\phi_S^S(x_3)]$$
$$\times \alpha_s(t_{a2}) h_{a2}(\alpha_{a2}, \beta_{a2}, b_B, b_3) \exp[-S_B(t_{a2}) - S_3(t_{a2})] S_t(x_3)$$
$$+ [4r(\bar{\eta} - x_B)\phi_S^S(x_3) + 2\bar{\eta}\phi_S(x_3)]\alpha_s(t_{b2}) h_{b2}(\alpha_{b2}, \beta_{b2}, b_3, b_B) \exp[-S_B(t_{b2}) - S_3(t_{b2})] S_t(x_B)\}. \tag{A14}$$

The nonfactorizable diagrams in Figs. 1(c2) and 1(d2) yield

(1) $(V - A)(V - A)$

$$M_c'^{LL} = \frac{4\pi C_F M_B^4}{\sqrt{2N_c}} \int_0^1 dx_B dz dx_3 \int_0^\infty b_B db_B b db \phi_B(x_B, b_B) \phi_S(z)$$
$$\times \{[4\bar{\eta}^2(x_B - z)\phi_S(x_3) + 4r(x_3\bar{\eta} + \eta\bar{z} - \bar{x}_B)(\phi_S^S(x_3) - \phi_S^T(x_3)) + 8r\eta(x_B - z)\phi_S^T(x_3)]$$
$$\times \alpha_s(t_{c2}) h_{c2}(\alpha_{c2}, \beta_{c2}, b, b_B) \exp[-S_B(t_{c2}) - S(t_{c2}) - S_3(t_{c2})]$$
$$+ [4\bar{\eta}(\bar{z} + \bar{x}_B - x_3\bar{\eta})\phi_S(x_3) + 4r(x_3\bar{\eta} - \eta\bar{z} - \bar{x}_B)(\phi_S^S(x_3) - \phi_S^T(x_3)) + 8r(1 - x_3\bar{\eta})\phi_S^T(x_3)]$$
$$\times \alpha_s(t_{d2}) h_{d2}(\alpha_{d2}, \beta_{d2}, b, b_B) \exp[-S_B(t_{d2}) - S(t_{d2}) - S_3(t_{d2})]\}. \tag{A15}$$

(2) $(V - A)(V + A)$

$$M_c'^{LR} = \frac{4\pi C_F M_B^4}{\sqrt{2N_c}} \int_0^1 dx_B dz dx_3 \int_0^\infty b_B db_B b db \phi_B(x_B, b_B)$$
$$\times \{[4\sqrt{(1 - r^2)}\eta(\bar{x}_3\bar{\eta} + z - x_B)(\phi_S^S(x_3) - \phi_S^T(x_3))(\phi_S^s(z) - \phi_S^t(z)) - 8\sqrt{(1 - r^2)}\eta r(x_B - z)$$
$$\times \phi_S^t(z)(\phi_S^S(x_3) - \phi_S^T(x_3)) + 8\sqrt{(1 - r^2)}\eta r\bar{x}_3\bar{\eta}\phi_S^T(x_3)(\phi_S^s(z) - \phi_S^t(z)) - 4\sqrt{(1 - r^2)}\eta\bar{\eta}(x_B - z)$$
$$\times \phi_S(x_3)(\phi_S^s(z) - \phi_S^t(z)) + 8\sqrt{(1 - r^2)}\eta\bar{\eta}(x_B - z)\phi_S(x_3)\phi_S^t(z)]\alpha_s(t_{c2}) h_{c2}(\alpha_{c2}, \beta_{c2}, b, b_B)$$
$$\times \exp[-S_B(t_{c2}) - S(t_{c2}) - S_3(t_{c2})] + [4\sqrt{(1 - r^2)}\eta r(x_3\bar{\eta} - \bar{x}_B - \bar{z})(\phi_S^S(x_3) - \phi_S^T(x_3))(\phi_S^s(z) - \phi_S^t(z))$$
$$- 8\sqrt{(1 - r^2)}\eta r(1 - x_3\bar{\eta})\phi_S^t(z)(\phi_S^S(x_3) - \phi_S^T(x_3)) - 8\sqrt{(1 - r^2)}\eta r(x_B - \bar{z})\phi_S^T(x_3)(\phi_S^s(z) - \phi_S^t(z))$$
$$+ 4\sqrt{(1 - r^2)}\eta\bar{\eta}(\bar{z} - x_B)\phi_S(x_3)(\phi_S^s(z) - \phi_S^t(z)) + 8\sqrt{(1 - r^2)}\eta(1 - x_3\bar{\eta})\phi_S(x_3)\phi_S^t(z)]$$
$$\times \alpha_s(t_{d2}) h_{d2}(\alpha_{d2}, \beta_{d2}, b, b_B) \exp[-S_B(t_{d2}) - S(t_{d2}) - S_3(t_{d2})]\}. \tag{A16}$$

(3) $(S - P)(S + P)$

$$M_c'^{SP} = \frac{-8\pi C_F M_B^4}{\sqrt{2N_c}} \int_0^1 dx_B dz dx_3 \int_0^\infty b_B db_B b db \phi_B(x_B, b_B) \phi_S(z)$$
$$\times \{[2\bar{\eta}(\bar{x}_3\bar{\eta} + z - x_B)\phi_S(x_3) - 2r(\eta(x_B - z) - \bar{x}_3\bar{\eta})(\phi_S^S(x_3) - \phi_S^T(x_3)) + 4r\bar{x}_3\bar{\eta}\phi_S^T(x_3)]$$
$$\times \alpha_s(t_{c2}) h_{c2}(\alpha_{c2}, \beta_{c2}, b, b_B) \exp[-S_B(t_{c2}) - S(t_{c2}) - S_3(t_{c2})]$$
$$+ [2\bar{\eta}(1 + \eta)(x_B - z)\phi_S(x_3) + 2r(x_3\bar{\eta} - \eta(\bar{x}_B + \bar{z}) - 1)(\phi_S^S(x_3) - \phi_S^T(x_3)) + 4r\eta(z - \bar{x}_B)\phi_S^T(x_3)]$$
$$\times \alpha_s(t_{d2}) h_{d2}(\alpha_{d2}, \beta_{d2}, b, b_B) \exp[-S_B(t_{d2}) - S(t_{d2}) - S_3(t_{d2})]\}. \tag{A17}$$

The contributions of the factorizable annihilation diagrams in Figs. 1(e2) and 1(f2) are

(1) $(V-A)(V-A)$

$$
\begin{aligned}
F_e'^{LL} = 2\pi C_F f_B M_B^4 \int_0^1 dz dx_3 \int_0^\infty b db b_3 db_3
\end{aligned}
$$

$$
\begin{aligned}
&\times \{[-2\bar{z}\bar{\eta}\,\phi_S(x_3)\phi_S(z) + 4\sqrt{(1-r^2)}\eta r(2-z)\phi_S^S(x_3)\phi_S^s(z) + 4\sqrt{(1-r^2)}\eta rz\phi_S^S(x_3)\phi_S^t(z)] \\
&\times \alpha_s(t_{e2})h_{e2}(\alpha_{e2},\beta_{e2},b_3,b)\exp[-S_3(t_{e2})-S(t_{e2})]S_t(z) \\
&+ [2\bar{\eta}(\eta+x_3\bar{\eta})\phi_S(x_3)\phi_S(z) - 4\sqrt{(1-r^2)}\eta r(1+x_3\bar{\eta}+\eta)\phi_S^S(x_3)\phi_S^s(z) + 4\sqrt{(1-r^2)}\eta r\bar{x}_3\bar{\eta} \\
&\times \phi_S^T(x_3)\phi_S^s(z)]\alpha_s(t_{f2})h_{f2}(z,x_3,b,b_3)\exp[-S_3(t_{f2})-S(t_{f2})]S_t(x_3)\}.
\end{aligned} \tag{A18}
$$

(2) $(V-A)(V+A)$

$$
F_e'^{LR} = F_e'^{LL} \tag{A19}
$$

$$
\begin{aligned}
F_e'^{SP} = -4\pi C_F f_B M_B^4 \int_0^1 dz dx_3 \int_0^\infty b db b_3 db_3
\end{aligned}
$$

$$
\begin{aligned}
&\times \{[-2\sqrt{(1-r^2)}\eta\bar{z}\phi_S(x_3)(\phi_S^s(z)-\phi_S^t(z)) - 4\sqrt{(1-r^2)}\eta\bar{z}\bar{\eta}\,\phi_S(x_3)\phi_S^t(z) + 4r(1+\eta\bar{z}) \\
&\times \phi_S^S(x_3)\phi_S(z)]\alpha_s(t_{e2})h_{e2}(\alpha_{e2},\beta_{e2},b_3,b)\exp[-S_3(t_{e2})-S(t_{e2})]S_t(z) \\
&+ [-4\sqrt{(1-r^2)}\eta\bar{\eta}\phi_S(x_3)\phi_S^s(z) + 2r(x_3\bar{\eta}+2\eta)\phi_S(z)(\phi_S^S(x_3)-\phi_S^T(x_3)) + 4r\eta\phi_S(z)\phi_S^T(x_3)] \\
&\times \alpha_s(t_{f2})h_{f2}(\alpha_{f2},\beta_{f2},b,b_3)\exp[-S_3(t_{f2})-S(t_{f2})]S_t(x_3)\}.
\end{aligned} \tag{A20}
$$

The contributions of the nonfactorizable annihilation diagrams in Figs. 1(g2) and 1(h2) are
(1) $(V-A)(V-A)$

$$
\begin{aligned}
M_g'^{LL} = \frac{-4\pi C_F M_B^4}{\sqrt{2N_c}} \int_0^1 dx_B dz dx_3 \int_0^\infty b_B db_B b db \phi_B(x_B,b_B)
\end{aligned}
$$

$$
\begin{aligned}
&\times \{[4\bar{\eta}((2-z)\eta+x_3\bar{\eta}-x_B)\phi_S(z)\phi_S(x_3) + 4\sqrt{(1-r^2)}\eta r(\bar{z}+x_3\bar{\eta}+\eta-x_B)(\phi_S^T(x_3)\phi_S^t(z) \\
&- \phi_S^S(x_3)\phi_S^s(z)) + 4\sqrt{(1-r^2)}\eta r(\bar{z}-x_3\bar{\eta}-\eta+x_B)(\phi_S^T(x_3)\phi_S^s(z)-\phi_S^S(x_3)\phi_S^t(z))] \\
&\times \alpha_s(t_{g2})h_{g2}(\alpha_{g2},\beta_{g2},b_B,b)\exp[-S_B(t_{g2})-S(t_{g2})-S_3(t_{g2})] \\
&+ [4(z\bar{\eta}(1+\eta)+r_b\bar{\eta})\phi_S(z)\phi_S(x_3) - 4\sqrt{(1-r^2)}\eta r(x_B-z-\bar{x}_3\bar{\eta})(\phi_S^T(x_3)\phi_S^t(z) \\
&- \phi_S^S(x_3)\phi_S^s(z)) - 4\sqrt{(1-r^2)}\eta r(x_B+z-\bar{x}_3\bar{\eta})(\phi_S^T(x_3)\phi_S^s(z)-\phi_S^S(x_3)\phi_S^t(z)) + 16\sqrt{(1-r^2)}\eta r_b r \\
&\times \phi_S^S(x_3)\phi_S^s(z)]\alpha_s(t_{h2})h_{h2}(\alpha_{h2},\beta_{h2},b_B,b)\exp[-S_B(t_{h2})-S(t_{h2})-S_3(t_{h2})]\}.
\end{aligned} \tag{A21}
$$

(2) $(V-A)(V+A)$

$$
M_g'^{LR} = \frac{-4\pi C_F M_B^4}{\sqrt{2N_c}} \int_0^1 dx_B dz dx_3 \int_0^\infty b_B db_B b db \phi_B(x_B, b_B)
$$

$$
\times \{[4\sqrt{(1-r^2)}\eta \bar{z}\,\bar{\eta}\,\phi_S(x_3)(\phi_S^s(z) - \phi_S^t(z)) - 8\sqrt{(1-r^2)}\eta r^2(x_B - \eta - x_3\bar{\eta})\phi_S(x_3)\phi_S^t(z) + 4r(\eta(2-z) - x_B
$$

$$
+ x_3\bar{\eta})\phi_S(z)(\phi_S^S(x_3) - \phi_S^T(x_3)) - 8r(x_B - \eta - x_3\bar{\eta})\phi_S^T(x_3)\phi_S(z)]\alpha_s(t_{g2})h_{g2}(\alpha_{g2}, \beta_{g2}, b_B, b)
$$

$$
\times \exp[-S_B(t_{g2}) - S(t_{g2}) - S_3(t_{g2})] + [4\sqrt{(1-r^2)}\eta\bar{\eta}(z + r_b)\phi_S(x_3)(\phi_S^s(z) - \phi_S^t(z)) - 4\sqrt{(1-r^2)}\eta(x_3\bar{\eta}
$$

$$
+ \eta\bar{z} - \bar{x}_B)\phi_S(z)(\phi_S^S(x_3) - \phi_S^T(x_3)) - 8\sqrt{(1-r^2)}\eta r^2(x_B - \bar{x}_3\bar{\eta} - r_b)\phi_S(x_3)\phi_S^t(z) + 8r
$$

$$
\times (x_B - \bar{x}_3\bar{\eta})\phi_S(x_3)\phi_S^t(z) + 4r(1 + \eta)\phi_S(z)(\phi_S^S(x_3) + \phi_S^T(x_3))]
$$

$$
\times \alpha_s(t_{h2})h_{h2}(\alpha_{h2}, \beta_{h2}, b_B, b) \exp[-S_B(t_{h2}) - S(t_{h2}) - S_3(t_{h2})]\}. \tag{A22}
$$

(3) $(S-P)(S+P)$

$$
M_g'^{SP} = \frac{8\pi C_F M_B^4}{\sqrt{2N_c}} \int_0^1 dx_B dz dx_3 \int_0^\infty b_B db_B b db \phi_B(x_B, b_B)
$$

$$
\times\{[-2\bar{z}\bar{\eta}(1 + \eta)\phi_S(x_3)\phi_S(z) + 2\sqrt{(1-r^2)}\eta r(x_3\bar{\eta} + \bar{z} - x_B + \eta)(\phi_S^S(x_3)\phi_S^s(z) - \phi_S^T(x_3)\phi_S^t(z))
$$

$$
+ 2\sqrt{(1-r^2)}\eta r(-x_3\bar{\eta} + \bar{z} + x_B - \eta)(\phi_S^T(x_3)\phi_S^s(z) - \phi_S^S(x_3)\phi_S^t(z))]\alpha_s(t_{g2})h_{g2}(\alpha_{g2}, \beta_{g2}, b_B, b)
$$

$$
\times \exp[-S_B(t_{g2}) - S(t_{g2}) - S_3(t_{g2})] + [2\bar{\eta}(x_3\bar{\eta} + \eta\bar{z} - \bar{x}_B + r_b)\phi_S(z)\phi_S(x_3) - 2\sqrt{(1-r^2)}\eta r
$$

$$
\times (x_B - z - \bar{x}_3\bar{z})(\phi_S^S(x_3)\phi_S^s(z) - \phi_S^T(x_3)\phi_S^t(z)) - 2\sqrt{(1-r^2)}\eta r(x_B + z - \bar{x}_3\bar{z})(\phi_S^T(x_3)\phi_S^s(z) - \phi_S^S(x_3)\phi_S^t(z))]
$$

$$
\times \alpha_s(t_{h2})h_{h2}(\alpha_{h2}, \beta_{h2}, b_B, b) \exp[-S_B(t_{h2}) - S(t_{h2}) - S_3(t_{h2})]\}. \tag{A23}
$$

The hard functions h_i are derived from the Fourier transform with $i = (a1, \ldots, h2)$, whose specific expressions are

$$
h_i(\alpha, \beta, b_1, b_2) = h_1(\alpha, b_1) \times h_2(\beta, b_1, b_2),
$$

$$
h_1(\alpha, b_1) = \begin{cases} K_0(\sqrt{\alpha}b_1), & \alpha > 0, \\ K_0(i\sqrt{-\alpha}b_1), & \alpha < 0, \end{cases}
$$

$$
h_2(\beta, b_1, b_2) = \begin{cases} \theta(b_1 - b_2)I_0(\sqrt{\beta}b_2)K_0(\sqrt{\beta}b_1) + (b_1 \leftrightarrow b_2), & \beta > 0, \\ \theta(b_1 - b_2)J_0(\sqrt{-\beta}b_2)K_0(i\sqrt{-\beta}b_1) + (b_1 \leftrightarrow b_2), & \beta < 0, \end{cases} \tag{A24}
$$

with the Bessel function J_0, the modified Bessel functions K_0 and I_0. The expressions for α and β in the hard functions are

$$\alpha_{(a1,b1)} = \beta_{(c1,d1)} = M_B^2 \bar{z}(1-r^2)(x_B - \eta),$$
$$\beta_{a1} = M_B^2(1 - \bar{\eta}(z + r^2\bar{z})),$$
$$\beta_{b1} = M_B^2(1-r^2)(x_B - \eta),$$
$$\alpha_{c1} = M_B^2(\bar{z}(1-r^2) + r^2 x_3)(x_B - \eta - x_3\bar{\eta}),$$
$$\alpha_{d1} = M_B^2(r^2(z - x_3) + \bar{z})(x_3\bar{\eta} - \bar{x}_B),$$
$$\alpha_{(e1,f1)} = \beta_{(g1,h1)} = M_B^2 \bar{x}_3\bar{\eta}(z(r^2 - 1) - r^2\bar{x}_3),$$
$$\beta_{e1} = M_B^2(r^2 x_3 - 1)(1 - x_3\bar{\eta}),$$
$$\beta_{f1} = M_B^2\bar{\eta}(-r^2\bar{z} - z),$$
$$\alpha_{g1} = M_B^2(z(1-r^2) + r^2\bar{x}_3)(x_B - \bar{x}_3\bar{\eta}),$$
$$\alpha_{h1} = M_B^2(1 + (\bar{z}(1-r^2) + r^2 x_3)(x_B - \eta - x_3\bar{\eta})),$$
$$\alpha_{(a2,b2)} = \beta_{(c2,d2)} = M_B^2 \bar{x}_3\bar{\eta}(x_B - r^2\bar{x}_3),$$
$$\beta_{a2} = M_B^2(1 - (1 - r^2\bar{x}_3)(x_3\bar{\eta} + \eta)),$$
$$\beta_{b2} = M_B^2\bar{\eta}(x_B - r^2),$$
$$\alpha_{c2} = M_B^2\bar{x}_3\bar{\eta}(x_B - z + r^2(z - \bar{x}_3)),$$
$$\alpha_{d2} = M_B^2(1 - x_3\bar{\eta})(r^2 x_3 + z(1-r^2) - \bar{x}_B),$$
$$\alpha_{(e2,f2)} = \beta_{(g2,h2)} = M_B^2(x_3\bar{\eta} + \eta)(-\bar{z}(1-r^2) - r^2 x_3),$$
$$\beta_{e2} = M_B^2(z(1-r^2) - 1),$$
$$\beta_{f2} = M_B^2(1 - r^2\bar{x}_3)(-\eta - x_3\bar{\eta}),$$
$$\alpha_{g2} = M_B^2(\bar{z}(1-r^2) + r^2 x_3)(x_B - \eta - x_3\bar{\eta}),$$
$$\alpha_{h2} = M_B^2(1 + (z(1-r^2) + r^2\bar{x}_3)(x_B - \bar{x}_3\bar{\eta})). \tag{A25}$$

The hard scales $t_i(i = a1, \ldots h2)$, which are taken to remove the large logarithmic radiative corrections, are given by

$$t_{a1} = \text{Max}\{\sqrt{|\beta_{a1}|}, 1/b_B, 1/b\}, \qquad t_{b1} = \text{Max}\{\sqrt{|\beta_{b1}|}, 1/b_B, 1/b\},$$
$$t_{c1} = \text{Max}\{\sqrt{|\alpha_{c1}|}, \sqrt{|\beta_{c1}|}, 1/b_B, 1/b_3\}, \qquad t_{d1} = \text{Max}\{\sqrt{|\alpha_{d1}|}, \sqrt{|\beta_{d1}|}, 1/b_B, 1/b_3\},$$
$$t_{e1} = \text{Max}\{\sqrt{|\beta_{e1}|}, 1/b, 1/b_3\}, \qquad t_{f1} = \text{Max}\{\sqrt{|\beta_{f1}|}, 1/b, 1/b_3\},$$
$$t_{g1} = \text{Max}\{\sqrt{|\alpha_{g1}|}, \sqrt{|\beta_{g1}|}, 1/b_B, 1/b_3\}, \qquad t_{h1} = \text{Max}\{\sqrt{|\alpha_{h1}|}, \sqrt{|\beta_{h1}|}, 1/b_B, 1/b_3\},$$
$$t_{a2} = \text{Max}\{\sqrt{|\beta_{a2}|}, 1/b_B, 1/b_3\}, \qquad t_{b2} = \text{Max}\{\sqrt{|\beta_{b2}|}, 1/b_B, 1/b_3\},$$
$$t_{c2} = \text{Max}\{\sqrt{|\alpha_{c2}|}, \sqrt{|\beta_{c2}|}, 1/b_B, 1/b\}, \qquad t_{d2} = \text{Max}\{\sqrt{|\alpha_{d2}|}, \sqrt{|\beta_{d2}|}, 1/b_B, 1/b\},$$
$$t_{e2} = \text{Max}\{\sqrt{|\beta_{e2}|}, 1/b, 1/b_3\}, \qquad t_{f2} = \text{Max}\{\sqrt{|\beta_{f2}|}, 1/b, 1/b_3\},$$
$$t_{g2} = \text{Max}\{\sqrt{|\alpha_{g2}|}, \sqrt{|\beta_{g2}|}, 1/b_B, 1/b\}, \qquad t_{h2} = \text{Max}\{\sqrt{|\alpha_{h2}|}, \sqrt{|\beta_{h2}|}, 1/b_B, 1/b\}. \tag{A26}$$

The Sudakov exponents are defined as

$$S_B = s(x_B p_1^+, b_B) + \frac{5}{3} \int_{1/b_B}^{t} \frac{d\bar{\mu}}{\bar{\mu}} \gamma_q(\alpha_s(\bar{\mu})),$$

$$S = s(z p^+, b) + s(\bar{z} p^+, b) + 2 \int_{1/b}^{t} \frac{d\bar{\mu}}{\bar{\mu}} \gamma_q(\alpha_s(\bar{\mu})),$$

$$S_3 = s(x_3 p_3^-, b_3) + s(\bar{x}_3 p_3^-, b_3) + 2 \int_{1/b_3}^{t} \frac{d\bar{\mu}}{\bar{\mu}} \gamma_q(\alpha_s(\bar{\mu})),$$

$$(A27)$$

with the anomalous dimension of the quark $\gamma_q = -\alpha_s/\pi$, and $s(Q, b)$ is the Sudakov factor, which can be found in Ref. [61]. Meanwhile, the threshold resummation factor $S_t(x)$ is taken from Ref. [62],

$$S_t(x) = \frac{2^{1+2c}\Gamma(\frac{3}{2} + c)}{\sqrt{\pi}\Gamma(1 + c)} [x(1 - x)]^c, \quad (A28)$$

with the parameter $c = 0.3$.

[1] N. N. Achasov and A. V. Kiselev, Light scalar mesons and two-kaon correlation functions, Phys. Rev. D **97**, 036015 (2018).

[2] P. Zyla *et al.* (Particle Data Group), Review of particle physics, Prog. Theor. Exp. Phys. **2020**, 083C01 (2020).

[3] H. Y. Cheng, C. K. Chua, and K. C. Yang, Charmless hadronic *B* decays involving scalar mesons: Implications on the nature of light scalar mesons, Phys. Rev. D **73**, 014017 (2006).

[4] E. M. Aitala *et al.* (Fermilab E791 Collaboration), Study of the $D_s^+ \to \pi^-\pi^+\pi^+$ Decay and Measurement of f_0 Masses and Widths, Phys. Rev. Lett. **86**, 765 (2001).

[5] D. C. Yan, X. Liu, and Z. J. Xiao, Anatomy of $B_s \to VV$ decays and effects of next-to-leading order contributions in the perturbative QCD factorization approach, Nucl. Phys. **B935**, 17 (2018).

[6] R. Zhou, Y. Li, and H. n. Li, Four-body decays $B_{(s)} \to (K\pi)_{S/P}(K\pi)_{S/P}$ in the perturbative QCD approach, J. High Energy Phys. 05 (2021) 82.

[7] Y. Li, D. C. Yan, R. Zhou, and Z. J. Xiao, Study of $B_{(s)} \to (\pi\pi)(K\pi)$ decays in the perturbative QCD approach, Eur. Phys. J. C **81**, 806 (2021).

[8] W. Liu and X. Q. Yu, Contributions of S-, P-, and D-wave resonances to the quasi-two-body decays $B_s^0 \to \psi(3686, 3770)K\pi$ in the perturbative QCD approach, Eur. Phys. J. C **82**, 441 (2022).

[9] W. F. Wang, H. C. Hu, H. n. Li, and C. D. Lü, Direct *CP* asymmetries of three-body *B* decays in perturbative QCD, Phys. Rev. D **89**, 074031 (2014).

[10] M. Diehl, T. Gousset, B. Pire, and O. Teryaev, Probing Partonic Structure in $\gamma^*\gamma \to \pi\pi$ near Threshold, Phys. Rev. Lett. **81**, 1782 (1998).

[11] M. Diehl, T. Gousset, and B. Pire, Exclusive production of pion pairs in $\gamma^*\gamma$ collisions at large Q^2, Phys. Rev. D **62**, 073014 (2000).

[12] C. H. Chen and H. n. Li, Vector-pseudoscalar two-meson distribution amplitudes in three-body *B* meson decays, Phys. Rev. D **70**, 054006 (2004).

[13] C. H. Chen and H. n. Li, Three-body nonleptonic B decays in perturbative QCD, Phys. Lett. B **561**, 258 (2003).

[14] B. Aubert *et al.* (BABAR Collaboration), Search for *B*-meson decays to two-body final states with $a_0(980)$ mesons, Phys. Rev. D **70**, 111102 (2004).

[15] B. Aubert *et al.* (BABAR Collaboration), Dalitz-plot analysis of the decays $B^\pm \to K^\pm \pi^\mp \pi^\pm$, Phys. Rev. D **72**, 072003 (2006).

[16] A. Garmash *et al.* (Belle Collaboration), Evidence for Large Direct *CP* Violation in $B^\pm \to \rho(770)^0 K^\pm$ from Analysis of Three-Body Charmless $B^\pm \to K^\pm \pi^\pm \pi^\pm$ Decays, Phys. Rev. Lett. **96**, 251803 (2006).

[17] P. Colangelo, F. De Fazio, and W. Wang, $B_s \to f_0(980)$ form factors and B_s decays into $f_0(980)$, Phys. Rev. D **81**, 074001 (2010).

[18] P. Colangelo, F. De Fazio, and W. Wang, Nonleptonic B_s to charmonium decays: Analysis in pursuit of determining the weak phase β_s, Phys. Rev. D **83**, 094027 (2011).

[19] R. Aaij *et al.* (LHCb Collaboration), First observation of $\bar{B}^0 \to J/\psi K^+K^-$ and search for $\bar{B}^0 \to J/\psi\phi$ decays, Phys. Rev. D **88**, 072005 (2013).

[20] A. Garmash *et al.* (Belle Collaboration), Study of three-body charmless B decays, Phys. Rev. D **65**, 092005 (2002).

[21] R. Zhou, Y. Q. Li, and J. Zhang, Isovector scalar $a_0(980)$ and $a_0(1450)$ resonances in the $B \to \psi(K\bar{K}, \pi\eta)$ decays, Phys. Rev. D **99**, 093007 (2019).

[22] J. Chai, S. Cheng, and A. J. Ma, Probing isovector scalar mesons in the charmless three-body B decays, Phys. Rev. D **105**, 033003 (2022).

[23] W. F. Liu, Z. T. Zou, and Y. Li, Charmless quasi-two-body B decays in perturbative QCD approach: Taking $B \to K(\mathcal{R} \to)K^+K^-$ as examples, Adv. High Energy Phys. **2022**, 5287693 (2022).

[24] L. Yang, Z. T. Zou, Y. Li, X. Liu, and C. H. Li, Quasi-two-body $B_{(s)} \to V\pi\pi$ decays with resonance $f_0(980)$ in the PQCD approach, Phys. Rev. D **103**, 113005 (2021).

[25] Z. R. Liang and X. Q. Yu, Perturbative QCD predictions for the decay $B_s^0 \to SS(a_0(980), f_0(980), f_0(500))$, Phys. Rev. D **102**, 116007 (2020).

[26] G. Buchalla, A. J. Buras, and M. E. Lautenbacher, Weak decays beyond leading logarithms, Rev. Mod. Phys. **68**, 1125 (1996).

[27] C. D. Lü, K. Ukai, and M. Z. Yang, Branching ratio and CP violation of $B \to \pi\pi$ decays in the perturbative QCD approach, Phys. Rev. D **63**, 074009 (2001).

[28] Y. Y. Keum, H. n. Li, and A. I. Sanda, Penguin enhancement and $B \to K\pi$ decays in perturbative QCD, Phys. Rev. D **63**, 054008 (2001).

[29] Y. Y. Keum, H. n. Li, and A. I. Sanda, Fat penguins and imaginary penguins in perturbative QCD, Phys. Lett. B **504,** 6 (2001).

[30] H. n. Li, Y. L. Shen, and Y. M. Wang, Resummation of rapidity logarithms in B meson wave functions, J. High Energy Phys. 02 (2013) 008.

[31] A. Ali, G. Kramer, Y. Li, C. D. Lü, Y. L. Shen, W. Wang, and Y. M. Wang, Charmless nonleptonic B_s decays to PP, PV, and VV final states in the perturbative QCD approach, Phys. Rev. D **76,** 074018 (2007).

[32] H. Y. Cheng, C. K. Chua, and K. C. Yang, Charmless B decays to a scalar meson and a vector meson Phys. Rev. D **77,** 014034 (2008).

[33] W. F. Wang, H. n. Li, W. Wang, and C. D. Lü, S-wave resonance contributions to the $B_{(s)}^0 \to J/\psi\pi^+\pi^-$ and $B_s \to \pi^+\pi^-\mu^+\mu^-$ decays, Phys. Rev. D **91,** 094024 (2015).

[34] U. G. Meißner and W. Wang, Generalized heavy-to-light form factors in light-cone sum rules, Phys. Lett. B **730,** 336 (2014).

[35] X. Ye and Z. P. Xing, S-wave contributions to $\bar{B}_s^0 \to (D^0, \bar{D}^0)\pi^+\pi^-$ in the perturbative QCD framework, Chin. Phys. C **43,** 073103 (2019).

[36] J. Back et al., Laura ++: A Dalitz plot fitter, Comput. Phys. Commun. **231,** 198 (2018).

[37] S. M. Flatte, Coupled-channel analysis of the $\pi\eta$ and $K\bar{K}$ systems near $K\bar{K}$ threshold, Phys. Lett. **63B,** 224 (1976).

[38] Z. T. Zou, L. Yang, Y. Li, and X. Liu, Study of quasi-two-body $B_{(s)} \to \phi(f_0(980)/f_2(1270) \to)\pi\pi$ decays in perturbative QCD approach, Eur. Phys. J. C **81,** 91 (2021).

[39] D. C. Yan, R. Zhou, Z. J. Xiao, and Y. Li, Study of $B_{(s)}^0 \to \phi\phi \to (K^+K^-)(K^+K^-)$ decays in the perturbative QCD approach, Phys. Rev. D **105,** 093001 (2022).

[40] R. Aaij et al. (LHCb Collaboration), Studies of the resonance structure in $D^0 \to K_S^0 K^\pm \pi^\mp$ decays, Phys. Rev. D **93,** 052018 (2016).

[41] W. F. Wang, Jian. Chai, and A. J. Ma, Contributions of $K_0^*(1430)$ and $K_0^*(1950)$ in the three-body decays $B \to K\pi h$, J. High Energy Phys. 03 (2020) 162.

[42] A. Abele et al., $\bar{p}p$ annihilation at rest into $K_L K^\pm \pi^\mp$, Phys. Rev. D **57,** 3860 (1998).

[43] R. Aaij et al. (LHCb Colloboration), Measurement of resonant and CP components in $\bar{B}_s^0 \to J/\psi\pi^+\pi^-$ decays, Phys. Rev. D **89,** 092006 (2014).

[44] H. Q. Liang and X. Q. Yu, Study of the four-body decays $B_S^0 \to \pi\pi\pi\pi$ in the perturbative QCD approach, Phys. Rev. D **105,** 096018 (2022).

[45] R. Aaij et al. (LHCb Colloboration), Analysis of the resonant components in $\bar{B}^0 \to J/\psi\pi^+\pi^-$, Phys. Rev. D **87,** 052001 (2013).

[46] A. Gokalp, Y. Sarac, and O. Yilmaz, An analysis of $f_0 - \sigma$ mixing in light cone QCD sum rules, Phys. Lett. B **609,** 291 (2005).

[47] H. Y. Cheng and K. C. Yang, $B \to f_0(980)K$ decays and subleading corrections, Phys. Rev. D **71,** 054020 (2005).

[48] X. Liu, Z. T. Zou, Y. Li, and Z. J. Xiao, Phenomenological studies on the $B_{d,s}^0 \to J/\psi f_0(500)[f_0(980)]$ decays, Phys. Rev. D **100,** 013006 (2019).

[49] M. Bargiotti et al. (OBELIX Collaboration), Coupled channel analysis of $\pi^+\pi^-\pi^0$, $K^+K^-\pi^0$ and $K^\pm K_S^0 \pi^\mp$ from $\bar{p}p$ annihilation at rest in hydrogen targets at three densities, Eur. Phys. J. C **26,** 371 (2003).

[50] C. Amsler et al. (Crystal Barrel Collaboration), Observation of a new $I^G(J^{PC}) = 1^-(0^{++})$ resonance at 1450 MeV, Phys. Lett. B **333,** 277 (1994).

[51] D. Barberis et al. (WA102 Collaboration), A measurement of the branching fractions of the $f_1(1285)$ and $f_1(1420)$ produced in central pp interactions at 450 GeV/c, Phys. Lett. B **440,** 225 (1998).

[52] H. Y. Cheng, Hadronic D decays involving scalar mesons, Phys. Rev. D **67,** 034024 (2003).

[53] A. V. Anisovich, V. V. Anisovich, and V. A. Nikonov, Radiative decays of basic scalar, vector and tensor mesons and the determination of the P-wave qmultiplet, Eur. Phys. J. A **12,** 103 (2001).

[54] N. Wang, Q. Chang, Y. L. Yang, and J. F. Sun, Study of the $B_s \to \phi f_0(980) \to \phi\pi^+\pi^-$ decay with perturbative QCD approach, J. Phys. G **46,** 095001 (2019).

[55] Q. X. Li, L. Yang, Z. T. Zou, Y. Li, and X. Liu, Calculation of the $B \to K_{0,2}^*(1430)f_0(980)/\sigma$ decays in the perturbative QCD approach, Eur. Phys. J. C **79,** 960 (2019).

[56] R. Fleischer, R. Knegjens, and G. Ricciardi, Anatomy of $B_{s,d}^0 \to J/\psi f_0(980)$, Eur. Phys. J. C **71,** 1832 (2011).

[57] M. Ablikim et al. (BES Collaboration), Evidence for $f_0(980)f_0(980)$ production in χ_{c0} decays, Phys. Rev. D **70,** 092002 (2004).

[58] M. Ablikim et al. (BES Collaboration), Partial wave analysis of $\chi_{c0} \to \pi^+\pi^- K^+K^-$, Phys. Rev. D **72,** 092002 (2005).

[59] K. M. Ecklund et al. (CLEO Collaboration), Study of the semileptonic decay $D_s^+ \to f_0(980)e^+\nu$ and implications for $B_s^0 \to J/\psi f_0$, Phys. Rev. D **80,** 052009 (2009).

[60] Z. R. Liang, F. B. Duan, and X. Q. Yu, Study of the quasi-two-body decays $B_s^0 \to \psi(3770)(\psi(3686))\pi^+\pi^-$ with perturbative QCD approach, Eur. Phys. J. C **79,** 370 (2019).

[61] H. n. Li and K. Ukai, Threshold resummation for non-leptonic B meson decays, Phys. Lett. B **555,** 197 (2003).

[62] T. Kurimoto, H. n. Li, and A. I. Sanda, Leading-power contributions to $B \to \pi, \rho$ transition form factors, Phys. Rev. D **65,** 014007 (2001).